ELSEVIER

Experimental Hematology

Experimental Hematology 2008;36:897–906

Growth and maturation of megakaryocytes is regulated by Lnk/Sh2b3 adaptor protein through crosstalk between cytokine- and integrin-mediated signals

Hitoshi Takizawa[a,c,*], Koji Eto[b], Atsuko Yoshikawa[c], Hiromitsu Nakauchi[b], Kiyoshi Takatsu[a,d,e], and Satoshi Takaki[c]

[a]*Division of Immunology, Department of Microbiology and Immunology;* [b]*Laboratory of Stem Cell Therapy, Center for Experimental Medicine, The Institute of Medical Science, The University of Tokyo, Tokyo, Japan;* [c]*Research Institute, International Medical Center of Japan, Tokyo, Japan;* [d]*Department of Immunobiology and Pharmacological Genetics, Graduate School of Medicine and Pharmaceutical Science for Research, University of Toyama, Toyama, Japan;* [e]*Prefectural Institute for Pharmaceutical Research, Toyama, Japan*

(Received 4 December 2007; revised 30 January 2008; accepted 7 February 2008)

Objective. **Various cytokines and growth factors control the differentiation and maturation of megakaryocytes (MKs). However, the mechanism regulating platelet release from MKs is not well understood. Here, we investigated a role of Lnk/Sh2b3, an intracellular adaptor protein, in megakaryopoiesis.**

Materials and Methods. **Number of MK progenitor in bone marrow (BM) of wild-type or *Lnk*$^{-/-}$ mice and their sensitivity to thrombopoietin (TPO) were determined in colony-forming unit assay. Using BM-derived wild-type or *Lnk*$^{-/-}$ MKs stimulated with TPO, activation of the signaling molecules was biochemically analyzed and effect of integrin stimulation on TPO signals was studied by addition of vascular cell adhesion molecule (VCAM-1). Platelet production from MKs in the presence of VCAM-1 was counted by flow cytometry and their morphological change was observed by time-lapse microscopy.**

Results. ***Lnk*$^{-/-}$ mice showed elevated platelets and mature MKs due to enhanced sensitivity of progenitors to TPO. Erk1/2 phosphorylation induced by TPO was augmented and prolonged in *Lnk*$^{-/-}$ MKs while activation of signal transducers and activators of transcription (Stat)3, Stat5, and Akt was normal. Wild-type MKs, but not in *Lnk*$^{-/-}$ MKs on VCAM-1 showed reduced Stat5 phosphorylation and mitogen-activated protein kinases activation upon stimulation with TPO. Additionally, the presence of VCAM in culture accelerated spontaneous platelet release from mature wild-type MKs, but not from *Lnk*$^{-/-}$ MKs.**

Conclusions. **Results suggest that contact of MKs with adhesion molecules via integrins might contribute to platelet release, which is under Lnk-mediated regulation of Stat-5 activation and show that Lnk functions in responses controlled by cell adhesion and in crosstalk between integrin- and cytokine-mediated signaling.** **© 2008 ISEH - Society for Hematology and Stem Cells. Published by Elsevier Inc.**

Megakaryocytes (MKs) and the platelets they produce are required for normal thrombosis and hemostasis [1]. Recent evidence indicates early roles of platelets in innate immune responses and tumor cell biology [2]. MK progenitors that reside in the bone marrow (BM) undergo endomitosis and differentiate into large, MKs with polyploidy in preparation for platelet production [3]. Thousands of platelets can be released from a single MK into the bloodstream. Thrombopoietin (TPO) is required for both MK development and maintenance of platelet production. Mutant mice lacking TPO or its receptor, c-Mpl, show severe thrombocytopenia [4,5]. However, the remaining platelets in those mice are morphologically and functionally normal [6]. Thus, the TPO/c-Mpl system plays a critical role in the survival and proliferation of MKs, but is not indispensable for either MK maturation or release of platelets.

*H. Takizawa's present address is Institute for Research in Biomedicine, 6500 Bellinzona, Switzerland.

Offprint requests to: Satoshi Takaki, M.D., Ph.D., Research Institute, International Medical Center of Japan, 1-21-1 Toyama, Shinjuku-Ku, Tokyo 162-8655, Japan; E-mail: stakaki@ri.imcj.go.jp

0301-472X/08 $–see front matter. Copyright © 2008 ISEH - Society for Hematology and Stem Cells. Published by Elsevier Inc.
doi: 10.1016/j.exphem.2008.02.004

A critical step in thrombopoiesis is migration and adhesion of MKs to sinusoidal endothelial cells, where proplatelets elongate into the extravascular space [7–9]. The process is regulated by a variety of chemokines and cytokines as well as by adhesive interactions between adhesion molecules and extracellular matrix proteins. Mice lacking P-selectin, but not E-selectin, show increased numbers of interleukin (IL)-3–responsive MK progenitors and mature MKs with high ploidy [10]. A deficiency of platelet-endothelial cell adhesion molecule-1 leads to migration defects of MKs in response to stromal cell-derived factor-1 (SDF-1) and their increased adhesion to BM matrix proteins [11,12]. SDF-1 promotes localization of MK progenitors to the sinusoidal vascular zone in BM. This occurs through vascular cell adhesion molecule-1 (VCAM-1) and fibroblast growth factor-4 augmented very late antigen-4 (VLA-4)–mediated adhesion of MKs to endothelial cells, enhancing both MK survival and maturation [13]. These findings suggest pivotal roles of MK interaction with endothelial cells in BM via integrins and their ligands as well as cytokine-independent regulation in thrombopoiesis.

Lnk, recently designated as SH2B adaptor protein 3 (Sh2b3), belongs to an adaptor protein family composed of SH2-B (Sh2b1) and adaptor protein with PH and SH2 domains, APS (Sh2b2). Lnk negatively regulates lymphopoiesis and early hematopoiesis. *Lnk*-deficiency results in enhanced production of B cells partly due to enhanced signaling through c-Kit, and expansion as well as enhanced function of hematopoietic stem cells (HSCs) [14–16]. In addition, it appears that Lnk negatively controls erythropoietin- and TPO-dependent signals in erythropoiesis and thrombopoiesis [16–18]. Our previous study revealed that motility of hematopoietic progenitor cells on VCAM-1, an integrin ligand, was modulated by Lnk-mediated pathways [19]. Although the expansion of HSCs in $Lnk^{-/-}$ mice is largely TPO-dependent, it appears that the enhanced capability of $Lnk^{-/-}$ HSCs for repopulating irradiated host animals is not accomplished solely by a TPO-dependent pathway [20]. These observations suggest that Lnk might participate in control of integrin-mediated cell motility in addition to regulation of cytokine-dependent growth.

In this study, we investigated the possibility that Lnk might control thrombopoiesis by modulating integrin-mediated responses in addition to TPO-dependent growth signaling. Lnk specifically suppressed TPO-induced activation of Erk1/2, constraining the sensitivity of MKs to TPO. Costimulation of MKs with TPO and VCAM-1 resulted in downregulation of signal transducers and activators of transcription (Stat) 5 and upregulation of mitogen-activated protein kinase (MAPK) activation compared to stimulation by TPO alone. Those changes mediated by co-stimulation by TPO and VCAM-1 were not observed in MKs lacking Lnk. Our results revealed a formerly unrecognized regulatory mechanism in thrombopoiesis through integrin signaling and showed that Lnk modulates crosstalk between integrin-mediated signals and cytokine-induced signals.

Materials and methods

Mice and reagents

C57BL/6 mice were purchased from CLEA Japan (Tokyo, Japan). $Lnk^{-/-}$ mice [14–16] and green fluorescent protein (GFP) transgenic mice [21], both are on C57BL/6 background, were bred and maintained under specific pathogen-free conditions at the animal facility of the Institute of Medical Science, the University of Tokyo. Recombinant human TPO, mouse IL-3, and mouse IL-6 were purchased from Peprotech (London, UK). Mouse VCAM-1/Fc chimera was provided by R&D Systems (Minneapolis, MN, USA). Purified human fibrinogen was from American Diagnostica Inc. (Stamford, CT, USA). Human collagen type I was from Nycomed Pharma GmbH (Munich, Germany). Anti–β-actin (clone 2.1) was obtained from Sigma (St. Louis, MO, USA), while anti–phospho-Stat5 (pTyr694), anti–phospho-Stat3 (pTyr705), anti-Stat3, anti–phospho-Akt (Ser473), anti-Akt, anti–phospho-Erk1/2 (pThr202/pTyr204), anti-Erk1/2, anti–phospho-p38 (pThr180/pTyr182), and anti-p38 were purchased from Cell Signaling Technology (Danvers, MA, USA). Additional antibodies included anti-Stat5a and anti-Stat5b (Santa Cruz Biotechnologies Inc., Santa Cruz, CA, USA), and secondary antibodies, horseradish peroxidase–coupled goat anti-rabbit IgG and sheep anti-mouse IgG (Amersham Pharmacia Biotechnology). Anti-Lnk antibodies were generated [14,15].

Flow cytometric analysis

BM cells or splenocytes from wild-type and Lnk-deficient mice were harvested with Iscove's modified Eagle's medium (IMDM; GIBCO, Invitrogen, Grand Island, NY, USA) containing 2% fetal bovine serum (FBS), incubated with anti-FcRγ2 antibody (2.4G2) to block nonspecific binding and stained with fluorescein isothiocyanate or phycoerythrin-conjugated anti-CD41 (MWReg30; BD Biosciences, San Jose, CA, USA). The percentage of $CD41^+$ cells in total BM was determined with a FACSCalibur instrument (BD Biosciences), and the absolute number of $CD41^+$ MKs in BM or spleen was calculated. The ratio of GFP^+ platelets in total $CD41^+$ platelets was also determined by flow cytometry. For polyploidy analysis, BM cells directly harvested from wild-type and $Lnk^{-/-}$ mice were dissociated in CATCH buffer (Hank's balanced salt solution [GIBCO, Invitrogen], including 0.38% sodium citrate, 1 mM adenosine, and 2 mM theophylline) and stained with fluorescein isothiocyanate-CD41 antibody. To stain nuclei, the labeled cells were washed and incubated overnight in 100 μg/mL propidium citrate and 50 μg/mL RNase in 1% sodium citrate solution at 4°C and subjected to flow cytometric analysis. For MKs used in the following biochemical analysis and in vitro platelet formation, bone marrow cells were cultured for 3 days and the ploidies of MKs purified from the culture were analyzed by the same method as described.

Platelet count

Peripheral blood was taken from wild-type and Lnk-deficient mice retro-orbitally and platelet count was analyzed on the flow cytometer programmed with mouse-specific parameter (Sysmex, Hyogo, Japan).

In vivo turnover of platelets

Platelet-rich plasma from GFP transgenic mice or GFP transgenic $Lnk^{-/-}$ mice was separated by centrifugation of whole blood at 150*g* for 15 minutes without braking. One micrometer prostaglandin E_1 and 5 U/mL apyrase (Sigma) were added followed by centrifugation at 750*g* for 10 minutes. The platelet pellet was resuspended in modified Tyrode-HEPES buffer pH 7.4 (10 mM HEPES, 12 mM $NaHCO_3$, 138 mM NaCl, 5.5 mM glucose, 2.9 mM KCl, and 1 mM $MgCl_2$) and the concentration was determined on the flow cytometer (Sysmex). Resultant platelets (2.5×10^9) were intravenously injected into wild-type C57BL/6 mice or $Lnk^{-/-}$ mice. Peripheral blood was collected by plastic tip from the retro-orbital sinus of recipient mice at several time points and was incubated with biotinylated anti-CD41 and peridinin-chlorophyll-protein–conjugated streptavidin for 20 minutes at room temperature, and the percentage of GFP^+ platelets was determined on a FACSCalibur.

Immunohistochemistry

Freshly dissected nondecalcified femurs from 6- to 8-week-old wild-type C57BL/6 mice or $Lnk^{-/-}$ mice were embedded in 4% carboxymethyl cellulose (FINETEC, Fuchu, Japan) and snap-frozen in N-hexane chilled in a slurry of ethanol and dry ice. Sections were generated via Kawamoto's film method (Cryofilm transfer kit; FINETEC). The 150-μm–thick cryostat sections were first blocked with 5% FBS/phosphate-buffered saline and then stained with fluorescein isothiocyanate–conjugated anti-CD41 in blocking buffer. Cell nuclei were labeled with TO-PRO3 (Molecular Probes, Invitrogen). Sections were then mounted with PERMAFLUOR (Beckman Coulter, Fullerton, CO, USA), and confocal microscopic analysis was performed with an Olympus FV-500 confocal microscope.

In vitro colony assays

BM cells were flushed from femurs of wild-type or $Lnk^{-/-}$ mice with IMDM (GIBCO, Invitrogen) containing 2% FBS. Marrow cells (1×10^5) were cultured in double-chamber slides using MegaCult-C (Stem Cell Technologies, Vancouver, Canada) in the presence of different concentration (0, 0.1, 1, 10, and 100 ng/mL) of human TPO or 100 ng/mL TPO, 10 ng/mL mouse IL-3, and 20 ng/mL mouse IL-6. After 7 days of cultivation, slides were dehydrated in cold acetone for 5 minutes and colonies were stained for acetylcholinesterase activity with 5 mM sodium citrate solution, including 3 mM $CuSO_4$, 0.5 mM $K_3[Fe(CN)_6]$, and 75 mM Na_2HPO_4 (pH 6.0). Slides were scored microscopically, and megakaryocyte colonies were defined as colonies with at least three megakaryocytes.

Megakaryocyte culture and purification

Lineage-negative BM cells (depleted of cells expressing B220, CD3, Mac-1, Gr-1, and TER-119) were enriched using Hematopoietic Progenitor Cell Enrichment Set (BD Bioscience) following manufacturer's protocol. In brief, BM cells were labeled with a biotinylated cocktail of lineage-specific antibodies followed by Streptavidin-conjugated magnetic beads and lineage marker–negative (Lin^-) cells were collected using BD IMagnet. Lin^- cells (1×10^6) were incubated in IMDM containing 0.5% bovine serum albumin (BSA), 10 ng/mL human transferrin, human insulin, 1.6 μg/mL low density lipoprotein, 40 μM adenosine triphosphate, 40 μM uridine triphosphate, 40 μM cytidine triphosphate, 40 μM guanosine triphosphate (Sigma), 50 μM 2-mercaptoethanol, 29.2 μg/mL L-glutamine, 100 IU/mL penicillin, and 100 μg/mL streptomycin (GIBCO, Invitrogen), in the presence of 20 ng/mL or 2 ng/mL TPO for wild-type or $Lnk^{-/-}$ cells, respectively. After culturing for 3 days, mature MKs were harvested by low-speed centrifugation (120*g* for 10 minutes) and purified by gravity sedimentation through discontinuous BSA (0%/1.5%/3%) for 45 minutes at room temperature.

Immunoblotting

Purified mature MKs after 3-day cultivation were washed with IMDM and further incubated in the absence of TPO for 16 hours for starvation. Subsequently, cells were stimulated with 10 ng/mL TPO for 0, 10, 30, and 60 minutes, and lysed in RIPA buffer (0.1% sodium dodecyl sulfate, 1% Triton X-100, 1% sodium deoxycholate, 158 mM NaCl, 10 mM Tris-HCl, 1 mM ethylene glycol tetraacetic acid, 5 mM ethylene diamine tetraacetic acid, 100 U/mL aprotinin, 1 mM sodium vanadate, 10 mM sodium fluoride, 10 μg/mL leupeptin, and 2 mM phenylmethylsulfonyl fluoride). For integrin stimulation experiments, purified and starved MKs were stimulated with 10 ng/mL TPO and 50 μg/mL VCAM-1, fibrinogen or collagen type 1 in the presence of 2 mM manganese for 10 minutes and lysed. Thirty-five micrograms of total protein was subjected to immunoprecipitation and immunoblotting using anti-Lnk antibodies or other antibodies as described previously [14].

In vitro platelet formation

Twenty-four–well plates were precoated with 20 μg/mL mouse recombinant VCAM-1 overnight at 4°C and washed three times with MK-conditioned media. Purified mature MKs as described above were incubated on BSA- or VCAM-1–coated plates including 250 μL the conditioned media including 1 ng/mL TPO for 12 hours, and the culture supernatant was collected after addition of ethylene diamine tetraacetic acid at a final concentration of 10 mM. Flow-Count Fluorospheres (Beckman Coulter) were added and platelets gated on the same scatter properties as freshly prepared blood platelets were enumerated with a flow cytometer. For anti-integrin-α4 antibody treatment, purified cells were incubated with anti-CD49d, the α4 chain of the VLA-4 (PS/2; SouthernBiotech, Birmingham, AL, USA) at the concentration of 10 μg/mL for 30 minutes prior to the assay.

Proplatelet formation analysis

Harvested fetal liver cells (E13 to 15) were incubated in DMEM including 10% FBS, 100 IU/mL penicillin, 100 μg/mL streptomycin, and 29.2 μg/mL L-glutamine, in the presence of 20 ng/mL or 2 ng/mL TPO for wild-type or $Lnk^{-/-}$ cells. After 3 to 5 days of cultivation, mature MKs were purified as described and washed with Leibovitz's L-15 medium (GIBCO, Invitrogen). MKs in suspension were mounted in semi-solid medium including 20% Leibovitz's L-15, 80% MegaCult M-3234 (Stem Cell Technologies) and 1 ng/mL TPO in 35-mm Petri dishes with a 10-mm glass hole (Matsunami Glass, Osaka, Japan) coated with 10 μg/mL BSA or VCAM-1. Images of proplatelet formation were obtained using confocal microscopy in a CO_2 chamber (FV500; Olympus, Tokyo, Japan).

Results

Mature platelets are increased in the absence of Lnk, but showed normal turnover in circulation

Platelets develop from HSCs in the BM. HSCs give rise to multipotent progenitors, differentiate into committed MK progenitors, and then further proliferate and differentiate into mature MKs. Platelets released from mature MKs circulate throughout the body for several days, and are eventually captured and degraded by macrophages in the spleen and liver. TPO plays key roles in the proliferation and maturation of MK progenitors and megakaryocytes, as well as in the expansion of HSCs. Previous studies by this and other groups have demonstrated that Lnk negatively regulates TPO-dependent signals in megakaryocytic cells as well as in HSCs [17,20,22]. Velazquez et al. reported deregulated hematopoiesis including thrombocytosis in *Lnk*-deficient mice [16]. Furthermore, Tong et al. showed that various signaling molecules downstream of c-Mpl (the TPO receptor), such as Jak2 tyrosine kinase, Stat-5, Erk1/2, and Akt are all hyperactivated in *Lnk*-deficient MK progenitors [17].

We attempted to confirm those observations, and also to define the steps in thrombopoiesis, which were regulated by Lnk-dependent pathway(s). First, we examined expression of Lnk protein in MK-lineage cells, and found that substantial amounts of Lnk protein were expressed in MKs and maintained by mature platelets (Fig. 1A, and data not shown). The number of platelets in peripheral blood was increased nearly fivefold in *Lnk*-deficient mice compared with normal mice (Fig. 1B), consistent with previous observations by Velazquez et al. The absence of Lnk in mature platelets might change their survival and turnover rate in circulation. We assessed the half-life of platelets and the phagocytic function of macrophages by adoptive transfer. Platelet-rich fractions were prepared from the blood of GFP-transgenic mice or GFP-transgenic $Lnk^{-/-}$ mice, and transferred into *Lnk*-sufficient normal mice (Fig. 1C) or *Lnk*-deficient mice (Fig. 1D). In both conditions, transferred *Lnk*-deficient platelets disappeared from peripheral blood at almost the same rate as normal mature platelets. The survival of mature platelets in circulation as well as removal and degradation of old platelets by peripheral macrophages were not affected by the absence of Lnk.

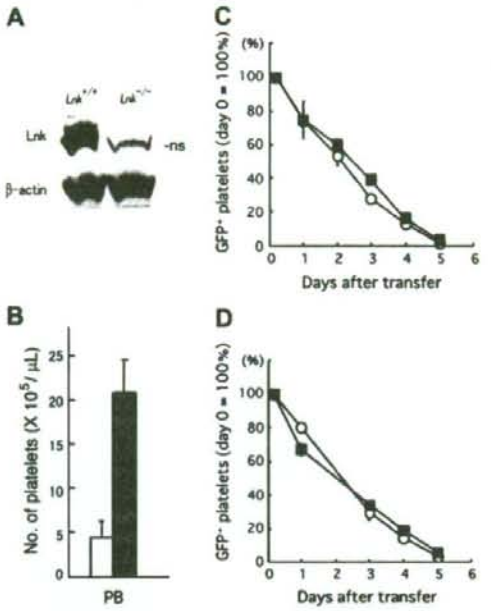

Figure 1. Lnk expression in megakaryocytes (MKs) and thrombocytosis in Lnk-deficient mice. (A) Substantial expression of Lnk in MKs. Lin^- cells obtained from bone marrow (BM) of $Lnk^{+/+}$ or $Lnk^{-/-}$ mice were cultured in the presence of 20 ng/mL or 2 ng/mL thrombopoietin (TPO), respectively. After a 3-day incubation, mature MKs were purified on density gradients and lysed. Total proteins were separated and immunoblotted with an anti-Lnk antibody (upper panel) or with an anti-actin antibody, as loading control (lower panel). NS = nonspecific band. (B) Fivefold increase in number of platelets in $Lnk^{-/-}$ mice. Peripheral blood was obtained retro-orbitally from $Lnk^{+/+}$ (open column) or $Lnk^{-/-}$ (closed column) mice and platelet counts were measured by flow cytometry. (C, D) Platelet turnover in $Lnk^{-/-}$ mice. Platelets obtained from green fluorescent protein-positive (GFP^+) wild-type (open circle) or GFP^+ $Lnk^{-/-}$ (closed square) mice were transferred to $Lnk^{+/+}$ (C) or $Lnk^{-/-}$ mice (D). Peripheral blood was taken from the recipient mice and the percentage of GFP^+ platelets was determined by flow cytometry. The relative percentage of GFP^+ platelets was calculated by dividing the percentage of GFP^+ platelets at each indicated time point by that at the day of transfer (Day 0).

Increased MK precursors in $Lnk^{-/-}$ mice and their distribution in BM

Next, we examined thrombopoiesis in the BM. $CD41^+$ MKs were significantly increased threefold in BM and nearly tenfold in the spleen (Fig. 2A). To determine whether MKs accumulated within specific regions of the BM of $Lnk^{-/-}$ mice, we undertook an immunohistochemical analysis. As shown in Figure 2B, numerous $CD41^+$ MKs were diffusely present throughout the BM in the femur in $Lnk^{-/-}$ mice, and no particular accumulating spot of $CD41^+$ cells was observed.

$Lnk^{-/-}$ MK precursors are hypersensitive to TPO and hypermature

The increase in MKs may be due to increased proliferation of progenitors and/or prolonged survival and maturation of MKs. Growth of MK progenitors and their sensitivity to TPO were evaluated by colony-forming assays. $Lnk^{-/-}$ progenitors formed colonies even at very low concentrations of TPO whereas normal progenitors hardly responded. Furthermore, the number of colony-forming cells upon full stimulation with TPO, IL-6, and IL-3 was twofold higher in $Lnk^{-/-}$ BM than in wild-type (Fig. 3A). Maturation of

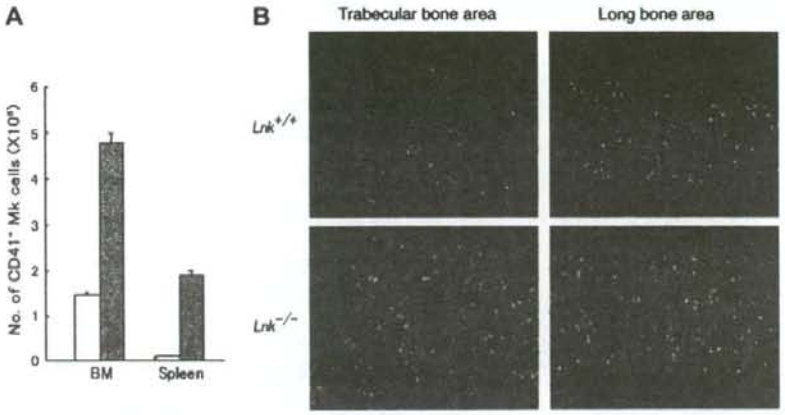

Figure 2. Megakaryocytes (MKs) numbers are increased in bone marrow (BM) and spleen of $Lnk^{-/-}$ mice. (A) Significant increase in MKs in BM and spleen. BM cells (left panel) or splenocytes (right panel) were harvested from $Lnk^{+/+}$ (open column) or $Lnk^{-/-}$ (closed column) mice and the percentage of $CD41^+$ MKs was determined by flow cytometry. The absolute number of $CD41^+$ MKs in each tissue was calculated by multiplying the percentage by the absolute number of total mononuclear cells. Shown are mean ± SD of results obtained from two experiments. (B) Immunofluorescence microscopic analysis of $Lnk^{-/-}$ BM. Frozen sections of femurs from $Lnk^{+/+}$ (upper) or $Lnk^{-/-}$ (lower) mice were stained with anti-CD41 (green) and TO-PRO3 (blue) and observed in confocal microscopy. Representative images of trabecular bone (left column) and long bone regions (right column) are shown.

MKs in BM also was quantified by measuring their ploidies. Polyploidy analysis of MKs in BM using flow cytometry showed that mature MKs with high polyploidy (32N and 64N) were more frequent in $Lnk^{-/-}$ BM. In contrast, a majority of MKs in normal BM had 16 nuclei (Fig. 3B). These data indicate that Lnk regulates the proliferation of MK progenitors by limiting their sensitivity to TPO, and *Lnk*-deficiency promoted expansion of MK-lineage cells. It seemed that Lnk also played a role in controlling maturation of MKs.

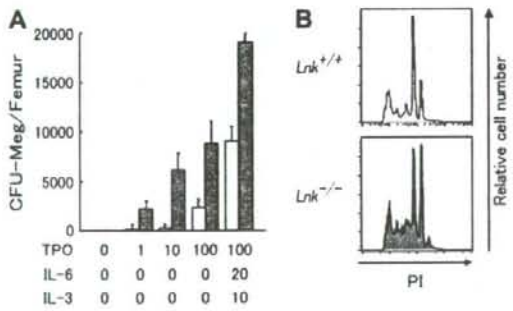

Figure 3. Megakaryocytosis in $Lnk^{-/-}$ mice. (A) Increased number of megakaryocytes (MK) progenitors and their hypersensitivity to thrombopoietin (TPO). Total bone marrow (BM) cells obtained from the BM of $Lnk^{+/+}$ (open column) or $Lnk^{-/-}$ (closed column) mice were cultured at the indicated concentration of TPO, interleukin (IL)-3, and IL-6 for 7 days. The mean ± SD of the number of colonies per femur are shown from three independent experiments. (B) BM cells of $Lnk^{+/+}$ (upper column) or $Lnk^{-/-}$ (lower column) mice were analyzed for DNA content. Representative data of multiple experiments are shown.

Lnk-deficiency causes augmented MAPK activation in MKs upon stimulation with TPO

To understand the molecular mechanism by which Lnk regulates TPO-induced MK proliferation, we examined overall protein phosphorylation following TPO stimulation using BM-derived MKs. We generated MKs with the same ploidy from wild-type and $Lnk^{-/-}$ mice by adjusting TPO concentration to levels that induced relatively comparable proliferative responses, and used them for biochemical analyses (Fig. 4A). Purified MKs were starved for 16 hours in TPO-free medium, stimulated with 10 ng/mL TPO and then lysed at several time points. The cell lysates were subjected to immunoblotting analyses for signaling molecules activated and phosphorylated downstream of c-Mpl (Fig. 4B). Stat3 and Akt was phosphorylated ten minutes after TPO stimulation and lasted >60 minutes in wild-type cells. Activation of Stat5, p38, and Erk1/2 was transiently observed, with peak phosphorylation 10 minutes after TPO stimulation. In $Lnk^{-/-}$ MKs, Erk1/2 activation was prolonged while phosphorylation levels of the other signaling molecules were essentially comparable to those induced in wild-type cells. Thus, our results indicated that Lnk specifically inhibited activation or regulates inactivation of Erk1/2 in TPO-dependent (c-Mpl–mediated) signaling pathways in MKs.

Megakaryocytic responses to combined exposure to TPO and integrins are modulated by expression of Lnk

Our previous study showed that the motility of hematopoietic progenitor cells on VCAM-1 was regulated by Lnk-mediated pathways [19]. We, therefore, asked whether

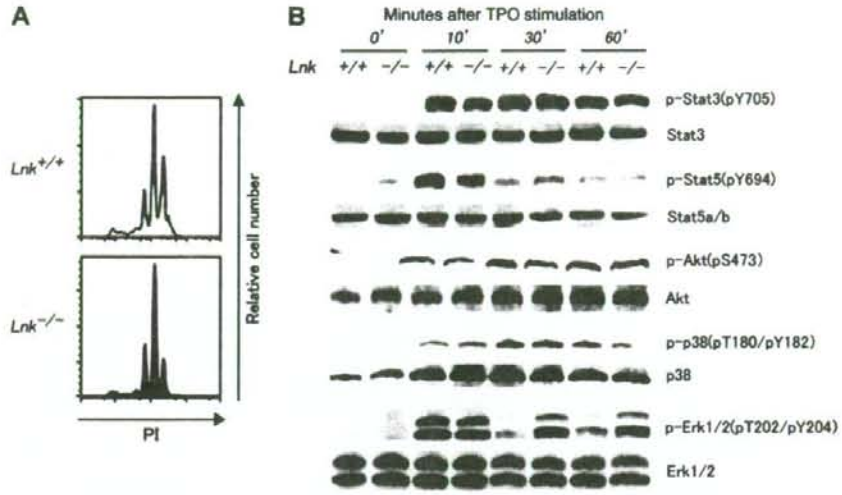

Figure 4. Thrombopoietin (TPO)-mediated hyperactivation of Erk1/2 in $Lnk^{-/-}$ megakaryocytes (MKs). (**A**) Equivalent ploidy between $Lnk^{+/+}$ and $Lnk^{-/-}$ MKs. Lin^- populations harvested from $Lnk^{+/+}$ (upper column) or $Lnk^{-/-}$ (lower column) mice were cultured in the presence of 20 ng/mL or 2 ng/mL TPO, respectively. (**B**) Augmented phosphorylation of Erk1/2 in Lnk-deficiency. Purified mature MKs were starved for 16 hours in the absence of TPO and re-stimulated with 10 ng/mL TPO for the indicated period. Total cell lysates were subjected to immunoblotting using indicated antibodies. Typical results of three independent experiments are shown.

additional stimuli through integrins might affect TPO-mediated megakaryopoiesis. It was also important to determine whether Lnk might be involved in integrin-mediated signaling pathways in MKs. Phosphorylation of cellular proteins was examined in both wild-type and $Lnk^{-/-}$ MKs, which were exposed to VCAM-1 in the presence of TPO and manganese to activate integrins. In wild-type cells, costimulation with TPO and VCAM-1 significantly inhibited Stat5 phosphorylation, and enhanced activation of p38 and Erk1/2 (Fig. 5A). On the other hand, in $Lnk^{-/-}$ MKs, TPO-dependent Stat5 activation was clearly induced even in the presence of VCAM-1 costimulation, while p38 activation was not enhanced (Fig. 5A). These observations suggest that costimulation by integrin engagement changed the nature of signals downstream of c-Mpl in MKs. Downregulated activation of Stat5 by VCAM-1 as well as augmented activation of p38 and Erk1/2 by VCAM-1 seemed to require Lnk-mediated pathways.

Costimulation by VCAM-1 and TPO reduces the release of platelets by $Lnk^{-/-}$ MKs

VCAM-1 is a ligand for $\alpha4\beta1$ and $\alpha4\beta7$ integrins and is expressed mainly on endothelial cells [23,24]. Adhesive interaction between endothelial cells and MKs through the VLA-4/VCAM-1 axis promotes maturation of megakaryocytes [25]. To examine how VCAM-1–mediated changes in TPO-induced cellular responses affected certain MK functions, we evaluated platelet release from mature MKs in vitro. Purified MKs were incubated on BSA- or VCAM-1–coated plates for 12 hours, after which the number of released platelets was counted by flow cytometry. In the absence of TPO, wild-type and $Lnk^{-/-}$ MKs produced similar numbers of platelets on BSA- and VCAM-1–coated plates. In the presence of TPO, wild-type MKs on VCAM-1 released greater numbers of platelets than those on BSA. In contrast, the number of platelets released by TPO-stimulated $Lnk^{-/-}$ cells on VCAM-1 was comparable to that observed with BSA. The number of released platelets from $Lnk^{-/-}$ MKs was significantly lower than that from normal cells on VCAM-1 (Fig. 5B and Table 1). Pretreatment by anti-integrin-$\alpha4$ antibody completely abolished the difference in platelet production between $Lnk^{-/-}$ and wild-type cells on VCAM-1 (Fig. 5B). Apoptosis of MKs leads to generation of functional platelets [26]. There was, however, no difference in the percentage of apoptotic cells or their ploidy between wild type and $Lnk^{-/-}$ cells either on BSA- or VCAM-1–coated plate (data not shown).

We examined the possibility that reduced platelet formation by $Lnk^{-/-}$ MKs on VCAM was due to morphological changes in MKs. We generated proplatelet-forming MKs from wild-type and $Lnk^{-/-}$ fetal liver progenitors and monitored their morphological changes on BSA and VCAM-1 by time-lapse confocal microscopic analysis (Fig. 6). While the wild-type MKs elongated proplatelets with pseudopodia shape on BSA, they produced more branched proplatelets from firmly attached and well-expanded cell body on VCAM-1. $Lnk^{-/-}$ MKs on BSA showed proplatelet formation comparable to that of wild-type cells on BSA.

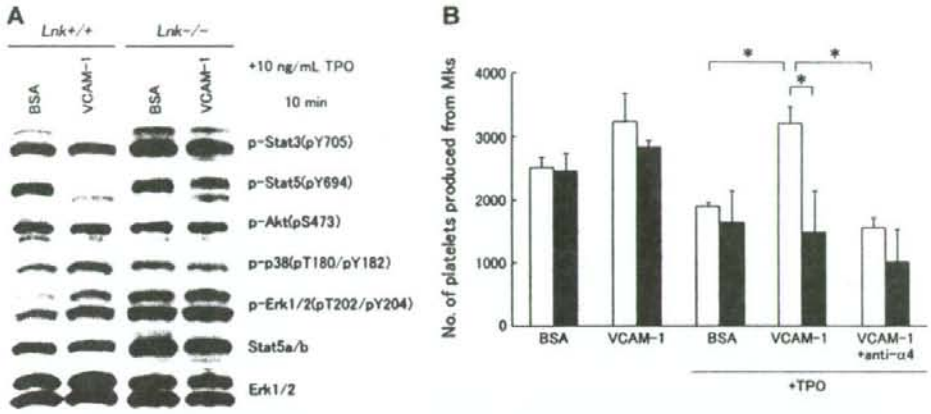

Figure 5. Changes of thrombopoietin (TPO)-induced cellular response by integrin ligands. **(A)** Modulation of TPO signaling pathways by integrin ligands. Mature megakaryocytes (MKs) obtained from $Lnk^{+/+}$ or $Lnk^{-/-}$ mice were starved for 16 hours without TPO and restimulated with both 10 ng/mL TPO and 50 μg/mL of vascular cell adhesion molecule-1 (VCAM-1). After 10 minutes incubation, cells were lysed and the lysates subjected to immunoblotting using the indicated antibodies. Results of several experiments are shown. **(B)** Augmented platelet production in the presence of VCAM-1. Purified $Lnk^{+/+}$ (open column) or $Lnk^{-/-}$ (closed column) MKs were incubated on either 20 μg/mL bovine serum albumin (BSA)- or VCAM-1–coated plates with or without addition of 1 ng/mL TPO for 12 hours. For anti-integrin-α4 antibody treatment, cells were preincubated with 10 μg/mL anti-CD49d for 30 minutes prior. The number of platelets was measured by flow cytometry. Shown are mean ± SD of results obtained from three independent experiments. *$p < 0.01$ comparison of $Lnk^{+/+}$ cells on VCAM-1–coated plates with that of $Lnk^{+/+}$ cells on BSA-coated plates, of $Lnk^{-/-}$ cells on VCAM-1–coated plates and of antibody-treated $Lnk^{+/+}$ cells on VCAM-1–coated plates.

However, $Lnk^{-/-}$ MKs on VCAM-1 developed proplatelets from not only the edge but also the center of the cell body with enlarged pseudopodial ends. This result suggests that a stimulation of integrin bound to VCAM-1 promoted platelet production by forming more proplatelets in wild-type MKs, and Lnk plays a role in regulating morphological changes for proplatelet formation.

Discussion

In this study, we demonstrated that $Lnk^{-/-}$ MK progenitors were hypersensitive to TPO, causing increased MK numbers, hypermaturation, and delayed platelet production on VCAM-1, which in turn led to thrombocytosis. It has been previously reported that *Lnk*-deficiency resulted in hyperactivation of TPO-dependent signaling molecules including Stat3, Stat5, Akt and Erk1/2 in MKs [17]. We also observed a significant enhancement in TPO-induced activation of Erk1/2 in $Lnk^{-/-}$ MKs, but not Stat3, Stat5 nor Akt in our experimental settings. The reasons for the discrepancy are currently unknown, but might be ascribed to the differences in the preparation of MKs used for biochemical analysis. Because the sensitivity of MKs to TPO declines during maturation and increase in ploidy [27], we prepared wild-type and $Lnk^{-/-}$ MKs with equalized ploidy and high purity from cultivated BM cells. MKs isolated by flow cytometric sorting from normal and *Lnk*-deficient mice might have different ploidy and purity because of low frequency and fragility of MKs in BM. Enhanced responses against other cytokines that activate Jak/Stat pathway, such as IL-3 or IL-7, have been suggested in the absence of Lnk. However, we did not observe any enhancements of cellular responses by IL-3, IL-7, and IL-5 in $Lnk^{-/-}$ precursors ([14,22] and unpublished observations). We believe that the inhibition of TPO-induced signals by

Table 1. VCAM-1 increases platelet release by megakaryocytes in the presence of Lnk

	Platelet production ratios in the presence of VCAM-1[a]	
	Genotype	
Cytokine addition	$Lnk^{+/+}$	$Lnk^{-/-}$
–TPO	1.19 ± 0.07	1.05 ± 0.18
+TPO	1.86 ± 0.15*	1.25 ± 0.27**

[a]Lin^- bone marrow (BM) precursor cells from wild-type or $Lnk^{-/-}$ mice were incubated for 3 days in the presence of 20 ng/mL or 2 ng/mL thrombopoietin (TPO), respectively. Purified megakaryocytes were incubated with or without 1 ng/mL TPO for an additional 12 hours. The number of platelets released in culture on vascular cell adhesion molecule (VCAM-1)–coated plates was counted by flow cytometry and compared with that on bovine serum albumin (BSA)–coated plates (see also Fig. 5B). Platelet production ratios were calculated by dividing the number of platelets on VCAM-1–coated membranes by that on BSA-coated membranes in the absence or presence of TPO. Data are presented as mean ± SD of results from three independent experiments.

*$p < 0.003$ compared with that of $Lnk^{-/-}$ in the presence of TPO or that of $Lnk^{+/+}$ in the absence of TPO.

**$p > 0.2$ compared with that of $Lnk^{-/-}$ in the absence of TPO.

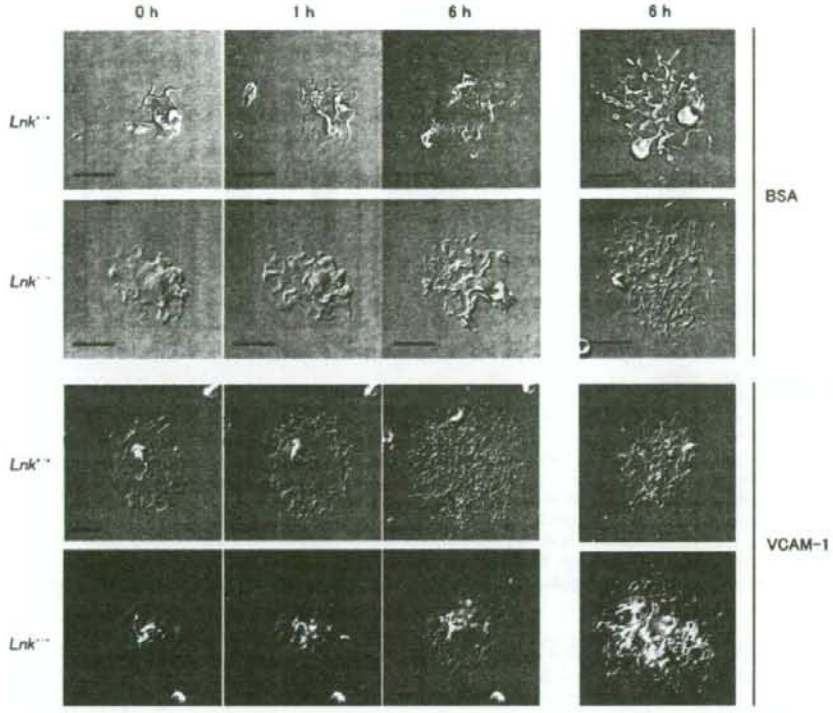

Figure 6. Morphological changes of $Lnk^{-/-}$ megakaryoctyes (MKs) producing proplatelets on vascular cell adhesion molecule-1 (VCAM-1). Fetal liver–derived $Lnk^{+/+}$ or $Lnk^{-/-}$ MKs were cultured on bovine serum albumin (BSA)– (upper panels) or VCAM-1–coated plates (lower panels) in microscope chambers and images were taken every hour up to 24 hours. Shown are representative images taken at the beginning of proplatelet elongation (0 hours), and following 3- and 6-hour observation. Images of another independent MKs at 6 hours were also shown. Scale bars: 50 μm.

Lnk involves cellular machinery specific to c-Mpl and does not act via Jak2 activation.

Our results revealed novel regulatory mechanisms in thrombopoiesis mediated by Lnk in addition to its role in constraining TPO signals. Additional stimulation by integrin ligand modulated TPO-induced signal responses of MKs. Engagement of integrin ligand induced strong mitogenic responses in MKs as well as in fibroblasts [28,29]. Interestingly, costimulation by TPO and VCAM-1 led to suppression of Stat5 phosphorylation and upregulation of p38 and Erk1/2 activation, which might change the nature of TPO-induced signals from ones supporting cell growth to those inducing cell-cycle arrest and differentiation. Consistently with this, we showed that normal MKs released greater numbers of platelets on VCAM-1 than on BSA. Administration of SDF-1 and fibroblast growth factor-4 to mice facilitates both MK maturation and platelet production by enhancing migration and adhesion of MK progenitors to BM endothelial cells through adhesion molecules including VCAM-1/VLA-4 [13]. Cellular interaction through VCAM-1 might trigger MKs to release platelets into the blood stream by terminating expression of Stat5-inducible genes after attachment of MKs to sinusoidal endothelial cells (Fig. 7A).

Inactivation of Stat5 was not observed in $Lnk^{-/-}$ MKs treated with TPO and VCAM-1. Additionally, platelet production from $Lnk^{-/-}$ MKs was not increased in the presence of VCAM-1. $Lnk^{-/-}$ MKs on VCAM-1 showed some morphological changes in proplatelet formation, which might be due to insufficient activation of demarcation membrane system of MKs [30], leading to inefficient platelet release in vitro upon integrin ligation by VCAM-1. In the absence of Lnk, MKs might continue undergoing endomitosis without producing platelets due to impaired Stat5 inactivation even if they contacted endothelial cells. This may lead to their hypermaturation in BM and result in more platelets production (Fig. 7B), because MKs with high ploidy are able to produce more platelets than those with low ploidy [31]. Thrombocytosis in $Lnk^{-/-}$ mice might be a consequence of increased numbers of MKs due to hypersensitivity of MK progenitors (TPO-dependent), in combination with accumulation of hypermature MKs attached

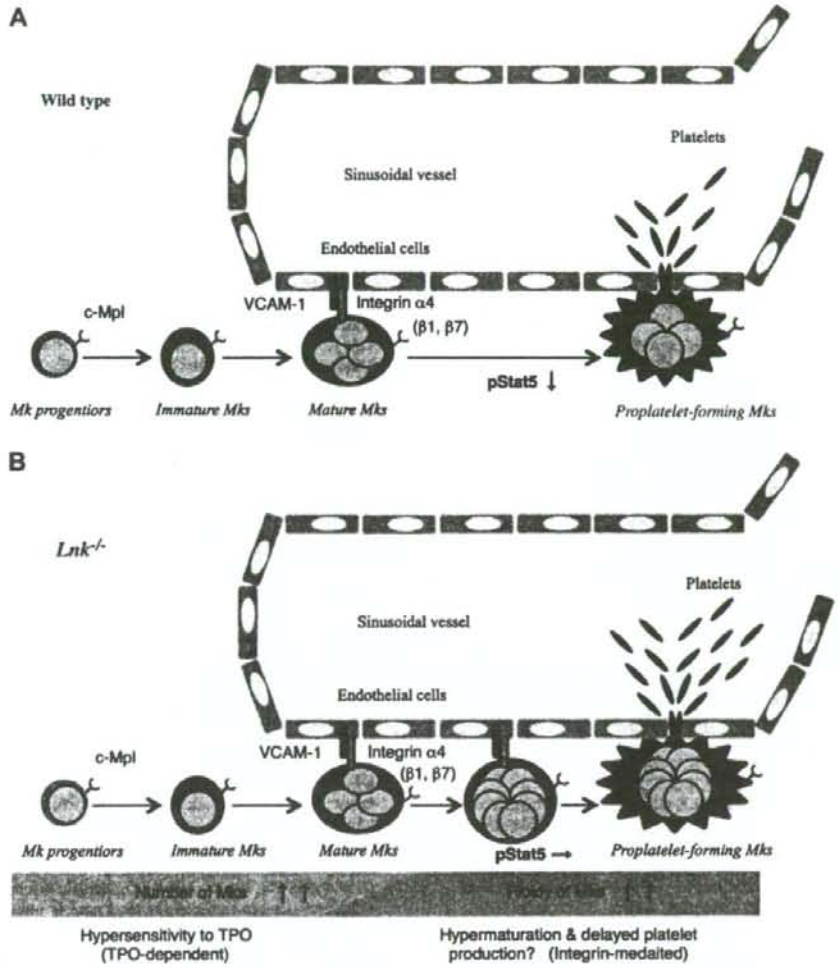

Figure 7. (A) Wild-type megakaryocytes (MK) progenitors proliferate and differentiate into mature MKs in response to thrombopoietin (TPO). When they contact the endothelial cells forming the sinusoidal vessels in bone marrow (BM) though integrinα4–vascular cell adhesion molecule-1 (VCAM-1) axis, platelets are released into bloodstream through proplatelet formation, which is possibly triggered by reduction of TPO-induced signal transducers and activators of transcription 5 (Stat5) activity upon VCAM-1 stimulation. (B) In the case of Lnk-deficiency, the number of mature MKs is increased due to enhanced sensitivity of $Lnk^{-/-}$ MK progenitor to TPO (TPO-dependent). After attaching the endothelial cell, MKs might keep undergoing endomitosis without platelet release, possibly due to impaired Stat5 inactivation, leading to their hypermaturation with an increase of ploidy.

to endothelial cells due to delayed platelet release (integrin-mediated) in Figure 7B. Future experiments will determine whether regulation of Stat5 is directly involved in initiation of platelet release, and how activation of Stat5 and MAPK in TPO-stimulated MKs is regulated by integrin- and Lnk-mediated events.

In summary, our results shed light on formerly unrecognized regulatory mechanisms in thrombopoiesis mediated by Lnk, and crosstalk between cytokines and integrins in MKs. TPO-induced Erk1/2 phosphorylation, but not activation of Stats and Akt, was constrained by Lnk, and was augmented in the absence of Lnk. Reduction of TPO-induced Stat5 and MAPKs activation in the presence of VCAM-1 co-ligation was mediated by a Lnk-dependent manner. Adhesion molecules play important roles in the biological properties of hematopoietic cells as environmental factors that determine cell fate. Understanding how integrin-mediated signals affect gene regulation or cytokine- or growth

factor–induced signaling pathways will be important to efforts to fully understand thrombopoiesis, hematopoiesis, and cellular responses.

Acknowledgments

We are grateful to our colleagues for helpful discussions, technical advices, and critical reading of this article. This work was supported by Grants-in-Aids from the Ministry of Education, Culture, Sports, Science and Technology, the Japanese Government. H.T is supported by Research Fellowship of the Japanese Society for the Promotion of Science for Young Scientists.

References

1. Kaushansky K. The molecular mechanisms that control thrombopoiesis. J Clin Invest. 2005;115:3339–3347.
2. Gupta GP, Massague J. Platelets and metastasis revisited: a novel fatty link. J Clin Invest. 2004;114:1691–1693.
3. Zimmet J, Ravid K. Polyploidy: occurrence in nature, mechanisms, and significance for the megakaryocyte-platelet system. Exp Hematol. 2000;28:3–16.
4. Gurney AL, Carver-Moore K, de Sauvage FJ, Moore MW. Thrombocytopenia in c-mpl-deficient mice. Science. 1994;265:1445–1447.
5. de Sauvage FJ, Carver-Moore K, Luoh SM, et al. Physiological regulation of early and late stages of megakaryocytopoiesis by thrombopoietin. J Exp Med. 1996;183:651–656.
6. Bunting S, Widmer R, Lipari T, et al. Normal platelets and megakaryocytes are produced in vivo in the absence of thrombopoietin. Blood. 1997;90:3423–3429.
7. Tavassoli M, Aoki M. Localization of megakaryocytes in the bone marrow. Blood Cells. 1989;15:3–14.
8. Zucker-Franklin D, Philipp CS. Platelet production in the pulmonary capillary bed: new ultrastructural evidence for an old concept. Am J Pathol. 2000;157:69–74.
9. Junt T, Schulze H, Chen Z, et al. Dynamic visualization of thrombopoiesis within bone marrow. Science. 2007;317:1767–1770.
10. Banu N, Avraham S, Avraham HK. P-selectin, and not E-selectin, negatively regulates murine megakaryocytopoiesis. J Immunol. 2002;169:4579–4585.
11. Dhanjal TS, Pendaries C, Ross EA, et al. A novel role for PECAM-1 in megakaryocytokinesis and recovery of platelet counts in thrombocytopenic mice. Blood. 2007;109:4237–4244.
12. Wu Y, Welte T, Michaud M, Madri JA. PECAM-1: a multifaceted regulator of megakaryocytopoiesis. Blood. 2007;110:851–859.
13. Avecilla ST, Hattori K, Heissig B, et al. Chemokine-mediated interaction of hematopoietic progenitors with the bone marrow vascular niche is required for thrombopoiesis. Nat Med. 2004;10:64–71.
14. Takaki S, Morita H, Tezuka Y, Takatsu K. Enhanced hematopoiesis by hematopoietic progenitor cells lacking intracellular adaptor protein. Lnk. J Exp Med. 2002;195:151–160.
15. Takaki S, Sauer K, Iritani BM, et al. Control of B cell production by the adaptor protein lnk. Definition of a conserved family of signal-modulating proteins. Immunity. 2000;13:599–609.
16. Velazquez L, Cheng AM, Fleming HE, et al. Cytokine signaling and hematopoietic homeostasis are disrupted in Lnk-deficient mice. J Exp Med. 2002;195:1599–1611.
17. Tong W, Lodish HF. Lnk inhibits Tpo-mpl signaling and Tpo-mediated megakaryocytopoiesis. J Exp Med. 2004;200:569–580.
18. Tong W, Zhang J, Lodish HF. Lnk inhibits erythropoiesis and Epo-dependent JAK2 activation and downstream signaling pathways. Blood. 2005;105:4604–4612.
19. Takizawa H, Kubo-Akashi C, Nobuhisa I, et al. Enhanced engraftment of hematopoietic stem/progenitor cells by the transient inhibition of an adaptor protein. Lnk. Blood. 2006;107:2968–2975.
20. Buza-Vidas N, Antonchuk J, Qian H, et al. Cytokines regulate postnatal hematopoietic stem cell expansion: opposing roles of thrombopoietin and LNK. Genes Dev. 2006;20:2018–2023.
21. Okabe M, Ikawa M, Kominami K, Nakanishi T, Nishimune Y. 'Green mice' as a source of ubiquitous green cells. FEBS Lett. 1997;407:313–319.
22. Seita J, Ema H, Ooehara J, et al. Lnk negatively regulates self-renewal of hematopoietic stem cells by modifying thrombopoietin-mediated signal transduction. Proc Natl Acad Sci U S A. 2007;104:2349–2354.
23. Imai K, Kobayashi M, Wang J, et al. Selective transendothelial migration of hematopoietic progenitor cells: a role in homing of progenitor cells. Blood. 1999;93:149–156.
24. Osborn L, Hession C, Tizard R, et al. Direct expression cloning of vascular cell adhesion molecule 1, a cytokine-induced endothelial protein that binds to lymphocytes. Cell. 1989;59:1203–1211.
25. Avraham H, Cowley S, Chi SY, Jiang S, Groopman JE. Characterization of adhesive interactions between human endothelial cells and megakaryocytes. J Clin Invest. 1993;91:2378–2384.
26. Clarke MC, Savill J, Jones DB, Noble BS, Brown SB. Compartmentalized megakaryocyte death generates functional platelets committed to caspase-independent death. J Cell Biol. 2003;160:577–587.
27. Paulus JM, Debili N, Larbret F, Levin J, Vainchenker W. Thrombopoietin responsiveness reflects the number of doublings undergone by megakaryocyte progenitors. Blood. 2004;104:2291–2298.
28. Morino N, Mimura T, Hamasaki K, et al. Matrix/integrin interaction activates the mitogen-activated protein kinase, p44erk-1 and p42erk-2. J Biol Chem. 1995;270:269–273.
29. Chen Q, Lin TH, Der CJ, Juliano RL. Integrin-mediated activation of MEK and mitogen-activated protein kinase is independent of Ras. J Biol Chem. 1996;271:18122–18127.
30. Schulze H, Korpal M, Hurov J, et al. Characterization of the megakaryocyte demarcation membrane system and its role in thrombopoiesis. Blood. 2006;107:3868–3875.
31. Mattia G, Vulcano F, Milazzo L, et al. Different ploidy levels of megakaryocytes generated from peripheral or cord blood CD34+ cells are correlated with different levels of platelet release. Blood. 2002;99:888–897.

Published July 28, 2008

Metalloproteinase regulation improves in vitro generation of efficacious platelets from mouse embryonic stem cells

Hidekazu Nishikii,[1] Koji Eto,[1] Noriko Tamura,[2] Koichi Hattori,[1] Beate Heissig,[1] Taisuke Kanaji,[3] Akira Sawaguchi,[4] Shinya Goto,[2] Jerry Ware,[5] and Hiromitsu Nakauchi[1]

[1]Division of Stem Cell Therapy, Center for Stem Cell and Regenerative Medicine, The Institute of Medical Science, University of Tokyo, Tokyo 108-8639, Japan
[2]Department of Medicine, Division of Cardiology, Tokai University School of Medicine, Isehara 259-1193, Japan
[3]Department of Medicine, Division of Hematology/Oncology, Kurume University School of Medicine, Fukuoka 830-0011, Japan
[4]Department of Anatomy, University of Miyazaki Faculty of Medicine, Miyazaki 889-1692, Japan
[5]Department of Physiology and Biophysics, University of Arkansas for Medical Sciences, Little Rock, AR 72205

Embryonic stem cells (ESCs) could potentially compensate for the lack of blood platelets available for use in transfusions. Here, we describe a new method for generating mouse ESC-derived platelets (ESPs) that can contribute to hemostasis in vivo. Flow cytometric sorting of cells from embryoid bodies on day 6 demonstrated that c-Kit$^+$ integrin αIIb (αIIb)$^+$ cells, but not CD31$^+$ cells or vascular endothelial cadherin$^+$ cells, are capable of megakaryopoiesis and the release of platelet-like structures by day 12. αIIbβ3–expressing ESPs exhibited ectodomain shedding of glycoprotein (GP)Ibα, GPV, and GPVI, but not αIIbβ3 or GPIbβ. ESPs showed impaired αIIbβ3 activation and integrin-mediated actin reorganization, critical events for normal platelet function. However, the administration of metalloproteinase inhibitors GM6001 or TAPI-1 during differentiation increased the expression of GPIbα, improving both thrombogenesis in vitro and posttransfusion recovery in vivo. Thus, the regulation of metalloproteinases in culture could be useful for obtaining high-quality, efficacious ESPs as an alternative platelet source for transfusions.

CORRESPONDENCE
Koji Eto:
keto@ims.u-tokyo.ac.jp
OR
Hiromitsu Nakauchi:
nakauchi@ims.u-tokyo.ac.jp

Abbreviations used: ADAM, a disintegrin and metalloproteinase; EB, embryoid body; ESC, embryonic stem cell; ESP, ESC-derived platelet; Flk, fetal liver kinase; GC, glycocalicin; GP, glycoprotein; HSC, hematopoietic stem cell; MMP, matrix metalloproteinase; PC, platelet concentrate; TEM, transmission electron microscopy; TIMP, tissue inhibitors of metalloproteinase; TPO, thrombopoietin; VE, vascular endothelial; VWF, von Willebrand factor.

Platelet concentrates (PCs) from donated blood are required to treat severe thrombocytopenia in patients with various hematological diseases, such as those who have undergone cancer chemotherapy or are recovering from hematopoietic stem cell (HSC) transplantation (1, 2). Frequent transfusion of PCs is clinically necessary because the half-life of transfused human platelets is 4–5 d (3). Platelets cannot be stored frozen, thus the ability to generate platelets in vitro would provide significant advances for platelet replacement therapy in clinical settings. A novel culture method to generate human platelets from cord blood CD34$^+$ cells was recently developed as an alternative source for PCs (4). However, technical difficulties in expanding ex vivo–cultured cord blood CD34$^+$ cells on a large scale have limited this as a reasonable in vitro approach for generating platelets.

Human embryonic stem cells (ESCs) can be forced to differentiate along a megakaryocytic lineage and represent a promising in vitro source for platelets. Owing to their pluripotency, ESCs can potentially proliferate indefinitely in culture (5). Platelets, as anucleate fragments of cytoplasm, can be irradiated before transfusion to effectively eliminate any contaminating cell, such as an undifferentiated ESC. The possibility of irradiation is important, as ESCs can potentially form teratomas or, if present at high numbers, elicit an immune response (6, 7). Thus, although ESCs represent a potentially safe and unlimited source of platelets in vitro, there are technical obstacles that remain.

First, culture methods for efficient in vitro generation of platelets have not been established.

The online version of this article contains supplemental material.

The Rockefeller University Press $30.00
J. Exp. Med. Vol. 205 No. 8 1917-1927
www.jem.org/cgi/doi/10.1084/jem.20071482

Published July 28, 2008

Second, appropriate in vivo function of the in vitro–produced platelet must be achieved. In addition, contamination with nonhuman antigens resulting in immunological reactions must be prevented. We and other groups have developed a method to generate large numbers of megakaryocytes and platelets from mouse ESCs grown on OP9 stromal cells in vitro (8, 9). However, these methods have not consistently produced ESC-derived megakaryocytes or platelets in sufficient quantity or quality to be considered as an alternative platelet source. No pre-selection for megakaryocyte progenitors was included in these previous reports. Studies have shown that the in vitro generation of large numbers of mature megakaryocytes depends on increased numbers of ESC-obtained progenitors (7, 8). Therefore, the identification and selection of megakaryocyte progenitors might increase the efficiency of megakaryopoiesis.

The functional platelet paradigm in hemostasis and thrombosis is the initiation of platelet adhesion to the extracellular matrix (10). One key event in this process is the interaction between glycoprotein (GP)Ibα (the platelet receptor) and von Willebrand factor (VWF) present in the extracellular matrix (10). Simultaneously, platelets can interact with surface-bound collagen via platelet receptors GPVI and integrin α2β1 (11). The net result is an activation of integrin αIIbβ3 to become a competent fibrinogen receptor leading to the formation of platelet aggregates (10). A recent report has also suggested that GPIbα contributes to arterial thrombosis in vivo independently of binding to VWF (12). Indeed, other studies have demonstrated that GPIbα associates with thrombin, kininogen, coagulation factors XI and XII, and thrombospondin-1 (13). In addition, the GPIb–V-IX complex, consisting of GPIbα, GPIbβ, GPIX, and GPV (10, 14), can bind integrin αMβ2 on macrophages/monocytes or P-selectin on endothelial cells (13). Of note, aged human and mouse platelets shed GPV and an extracellular domain of GPIbα, which contains the binding sites for VWF and thrombin (13, 15). This process involves the action of a disintegrin and metalloproteinase (ADAM)17 (also referred to as tumor necrosis factor α converting enzyme) (16). This leads to decreased platelet function (16, 17).

In this study, we demonstrate that c-Kit$^+$ integrin αIIb (αIIb)$^+$ cells isolated from ESCs differentiate with high efficiency into megakaryocytes and ESC-derived platelets (ESPs) in the presence of thrombopoietin (TPO) and stromal cells. We also show that ESPs shed extracellular domains of GPIbα, GPV, and GPVI in culture, reducing αIIbβ3 activation and actin polymerization. Consequently, these ESPs are functionally impaired in thrombus growth (18, 19). However, the inhibition of metalloproteinases restores platelet function, making ESPs from induced pluripotent stem cells a source of platelets with therapeutic potential (20, 21).

RESULTS

Markers defining megakaryocyte differentiation from ESCs

The cell markers defining the megakaryocytic lineage in a culture system of ESCs or HSCs are not understood. It is known that megakaryocyte progenitors are highly enriched in the CD9$^+$αIIb subunit$^+$ (αIIb$^+$)FcγR^{lo}c-Kit$^+$Sca-1$^-$Lin$^-$ fraction of bone marrow cells (22). The αIIb integrin subunit is an early primitive and definitive marker of hematopoiesis in the mouse embryo (17, 18) and a lineage-specific marker for postnatal megakaryocytes and platelets (23). We reasoned that CD31$^+$, αIIb$^+$, or c-Kit$^+$ cells were candidates for megakaryocyte progenitors derived from ESCs because postnatal HSCs, mature megakaryocytes, and platelets all express CD31 and αIIbβ3, and postnatal megakaryocyte progenitors express both c-Kit and αIIbβ3 (22).

To determine which cells actually contribute to megakaryopoiesis, we chose to induce a liquid culture system of ESCs for embryoid body (EB) formation (24). Sorted cells were then applied onto OP9 stromal cells to differentiate along the megakaryocytic lineage (Fig. 1 A). This two-stage approach was used because EB formation has been reported to be more suitable than co-culture with OP9 cells in producing hematopoietic progenitors in vitro (25). Indeed, liquid culture for EB formation resulted in reproducibly higher expression of the αIIb integrin subunit than the use of the OP9 co-culture system (Fig. 1 B) (26). ESCs co-cultured with OP9 stromal cells preferentially expressed CD31 (Fig. 1 B, right) or vascular endothelial (VE)-cadherin (unpublished data) by days 4–5, as reported (27).

To trace newly developed megakaryocytes and platelets in culture, we generated a novel ESC line in which the platelet-specific GPIbα promoter supports expression of a human GPIbα–EGFP fusion protein (Fig. 1 C, GPIb-ESCs) (28–30). Earlier reports showed selective expression in megakaryocytes and platelets using this system (29–31). The GFP-tagged cells were detectable by day 9 in the presence of TPO (Fig. 1 C). In addition, GFP expression was detectable only in αIIb$^+$GPIbα$^+$ megakaryocytes derived from cultures treated with TPO but not in Ter119$^+$ erythroblasts isolated from erythropoietin-containing cultures (not depicted). We further separated EB cells on day 6 to identify which fraction could differentiate into GFP-expressing megakaryocytes (Fig. 1 D). Murine ESCs (2×10^5 per 100-mm dish) typically produced 10^6 c-Kit$^+$αIIb$^+$ cells by day 6 and 2.5×10^6 αIIb$^+$ megakaryocytes by day 12. Cells derived from the c-Kit$^+$αIIb$^+$ fraction at day 6 expressed GFP on day 12 at 10-fold higher levels compared with cells in other fractions or in unfractionated whole EB-derived cells (Fig. 1 E). Fetal liver kinase (Flk)-1$^+$CD31$^+$ or VE-cadherin$^+$c-Kit$^+$ cells from day 6 EB did not contribute to megakaryopoiesis in this system (Fig. 1, D and E). ESC-derived VE-cadherin$^+$c-Kit$^+$CD45$^-$ cells in OP9 co-culture had been reported to contribute to definitive hematopoiesis (32).

Serial RT-PCR studies to detect GPIbα or GPV, both megakaryocytic-specific markers (33), along with the essential transcription factors for megakaryopoiesis, GATA-1, GATA-2, FOG-1, Fli-1, or NF-E2 (34, 35), indicated that day 6 EB c-Kit$^+$αIIb$^+$ cells were positive for these markers in the presence of TPO on OP9 stromal cells (Fig. 1 F) (34). Indeed, day 6 EB c-Kit$^+$αIIb$^+$ cells corresponded to CD9$^+$Sca-1$^-$ cells in bone marrow–derived megakaryocyte progenitors (Fig. 1 D) (22), and their morphological features resembled immature hematopoietic progenitor cells derived from adult bone marrow (Fig. 1 G) (22). We concluded from these results that

Published July 28, 2008

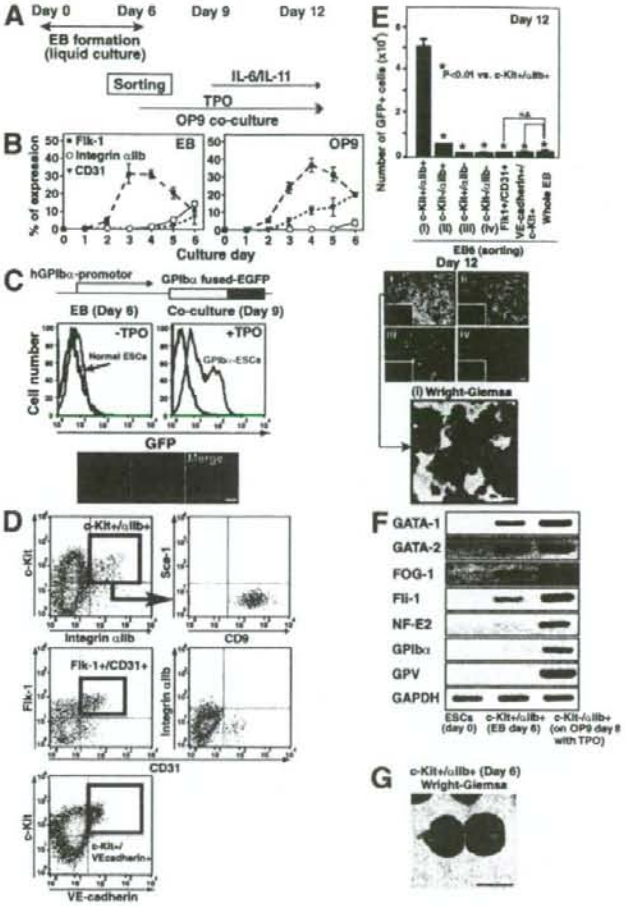

Figure 1. c-Kit⁺αIIb⁺ cell selection from day 6 EB determines the megakaryocytic lineage. (A) Protocol used in this study. (B) EB formation or OP9 co-culture was used for ESC differentiation from day 0 through day 6 in vitro. On the indicated days of culture, expression of Flk-1, integrin αIIb subunit (CD41), or CD31 was examined in both groups of cultured cells. The graph shows mean ± SEM from three independent experiments. (C) GPIbα and GFP expression in GPIbα-ESCs is regulated by the human GPIbα promoter. GFP is detectable in cultured cells that exhibit megakaryopoiesis (day 9) but not in progenitors (day 6). In the bottom box, cells with surface-expressed GFP also express human GPIbα. The cells on day 9 were fixed and stained to mark human GPIbα to confirm the colocalization with GFP expression at the membrane of the cells. Bars, 10 μm. (D) Representative dot plots for the expression of individual antigens on 10,000 living cells from day 6 EB. c-Kit⁺αIIb⁺ cells corresponded with Flk-1⁺ cells (not depicted) but not with VE-cadherin⁺ cells. And >96% of c-Kit⁺αIIb⁺ cells are found in the CD9⁺Sca-1⁻ fraction. (E) EB cells were sorted as shown in D, and 20,000 cells per well of a 6-well plate were seeded onto OP9 stroma cells in the presence of TPO. The left graph shows the number of generated GFP⁺ cells (mean ± SEM) per well of a 6-well plate on day 12 of culture. Representative images from day 12 culture dishes (phase or fluorescence microscopy [insets: bar, 50 μm] of four different fraction-derived cells at day 6; i, c-Kit⁺/αIIb⁺; ii, c-Kit⁻/αIIb⁺; iii, c-Kit⁺/αIIb⁻; iv, c-Kit⁻/αIIb⁻ [phase: bar, 50 μm]) and of Wright-Giemsa–stained cytospin preparation on day 12 derived from c-Kit⁺/αIIb⁺ fraction of day 6 were also shown. Bar, 50 μm. Results indicate that c-Kit⁺/αIIb⁺ fraction of day 6 (i) selectively yields megakaryocytes on day 12. Similar results have been obtained from three independent experiments. (F) Expression of genes related to the megakaryocytic lineage as determined by RT-PCR of cells from day 0, 6, or 8 cultures as indicated. (G) Wright-Giemsa–stained cytospin preparation of sorted c-Kit⁺αIIb⁺ cells from EB at day 6 is shown. Bar, 10 μm.

c-Kit⁺αIIb⁺ cells derived from ESCs can differentiate displaying several markers unique to the megakaryocytic lineage.

GPIbα expression on ESPs is reduced during in vitro culture

EB generation from ESC in liquid culture (6 d) followed by sorting for c-Kit⁺αIIb⁺ cells (Fig. 1 A) resulted in the constant generation of megakaryocytes and platelet-like particles, an improvement over our previously reported culture conditions (9). After 8–14 d in culture (2–8 d on co-culture with OP9 stromal cells), culture supernatants contained proplatelets (Fig. 2 A, i) and platelet-sized particles consistent with ESPs (Fig. 2 B). The granularity and size of these ESPs varied from those of

Published July 28, 2008

circulating murine platelets as determined by transmission electron microscopy (TEM) (Fig. 2 A) and the forward scatter profiles produced by flow cytometry (Fig. 2 B). Thus, the culture conditions seem to yield various developmental stages of a platelet (36). ESPs displayed an extensive surface-connected open canalicular system and multiple α or dense granules (Fig. 2 A, ii and iii). As compared with a normal mouse platelet, ESPs had a reduced number of granules per ESP (unpublished data).

We examined the relative expression of receptors by flow cytometry comparing ESPs and freshly isolated murine platelets. Expression of the integrin αIIb, GPIbβ, and GPIX was similar in platelets from the two sources (Fig. 2 B). However, expression of GP Ibα, GPV, and GPVI was significantly less for ESPs as compared with mouse platelets (Fig. 2 B). Cells with an $\alpha IIb^+GPIb\alpha^-GPIb\beta^+$ phenotype composed 35–65% of the cellular population after 12–14 d in culture. Reduced GPIbα expression of ESPs was not detected at day 8 (Figs. 2 C, i and ii), consistent with a longer time in culture leading to a loss of $GPIb\alpha^+$ cells or shedding of GPIbα from the cell. Unlike ESPs, ESC-derived megakaryocytes did not exhibit reduced GPIbα expression, even when cultured for >8 d (Fig. 2 C, i).

ADAM17 can cleave the extracellular domain of GPIbα on human and mouse platelets abrogating platelet function by its metalloproteinase activity (16, 17). Thus, we investigated whether a metalloproteinase supported the shedding of GPIbα in culture. Two potent metalloproteinase inhibitors, GM6001 (Ilomastat) or TAPI-1, were added to the co-culture system to evaluate the potential involvement of a matrix metalloproteinase (MMP). Because both inhibitors also inhibit MMP9, which has been reported to facilitate megakaryopoiesis (37), the drugs were administered only after day 10 (day 4 of co-culture) when megakaryocyte polyploidy is observed (9). Indeed, we found that the addition of GM6001 at the co-culture start impaired megakaryopoiesis (not depicted). GM6001 and TAPI-1 (Fig. 3 B, 1 and 10 μM) increased GPIbα expression on released ESPs at day 12 (Fig. 3, A and B). This increased expression did not affect the total number of αIIb^+ ESPs ($\alpha IIb^+GPIb\alpha^+$ plus $\alpha IIb^+GPIb\alpha^-$) at days 12 (Fig. 3 C) or 14 (not depicted). But the reduction of GPIbα was not observed on megakaryocytes during the culture (Figs. 2 C, i, and 3 A). Similarly, GM6001 addition to the culture restored expression of GPV and GPVI in αIIb^+ ESPs (Fig. 3 D) as reported

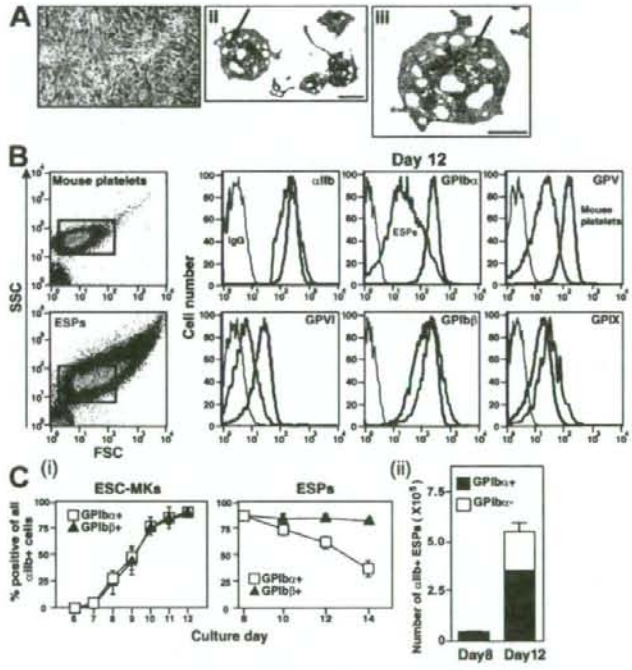

Figure 2. GPIbα expression is reduced on cultured ESPs but not megakaryocytes. (A) On day 12 of the culture, ESC-derived megakaryocytes bearing proplatelets are represented in panel (i) (phase contrast image in culture dish). Bar, 100 μm. Panels (ii) and (iii) show TEM images of ESPs. The subcellular structure of ESPs showed an open canalicular system, dense granules (arrowhead), and α granules (arrow), which were similar to those of peripheral blood platelets. Bars, 1 μm. (B) Mouse platelets (12 wk old) or ESPs (day 12) were subjected to flow cytometry. Graphs show representative forward scatter (FSC) or side scatter (SSC) dot plots. ESPs vary in size compared with mouse platelets. The remaining six graphs show surface expression of αIIb integrin subunit, GPIbα, GPIbβ, GPV, GPVI, and GPIX on mouse platelets (red lines) or ESPs (blue lines) with control IgG (black lines). (C) (i) On the indicated days of culture (x axis), expression of GPIbα and GPIbβ in αIIb+ megakaryocytes derived from ESCs and ESPs is shown. Panel (ii) shows the number of αIIb^+ ESPs on days 8 and 12 that are either $GPIb\alpha^+$ (black bar) or $GPIb\alpha^-$ (white bar). All results are mean ± SEM from four independent experiments.

Published July 28, 2008

for aged blood platelets (15, 38). These results suggest that metalloproteinase(s) impairs the retention of GPIbα, GPV, and GPVI on ESPs. Biochemical analysis confirmed that ESPs in culture shed the extracellular domain of GPIbα, referred to as "glycocalicin" (GC), in the absence of GM6001 but not in the presence of GM6001 (Fig. 3 E). As ESC-derived megakaryocytes do not show receptor shedding (Fig. 3, A and E, i), we removed them from the day 12 cell culture population. The remaining specimens were centrifuged, and pellets along with the corresponding supernatant were analyzed. Western blot analysis revealed GPIbα and GC antigen in the absence of GM6001, but a single band of GPIbα alone in the presence of GM6001 (Fig. 3 E, ii). A single band of GC was detectable only in the absence of GM6001 in ESP-derived supernatant (Fig. 3 E, iii).

To study whether pre-activation by plasma membrane injury or the activation state of ESPs is associated with metalloproteinase activity during culture, we examined the annexin V binding and P-selectin expression in the absence or presence of GM6001. Annexin V is a marker of platelet activation that detects the translocation of phosphatidylserine to the outer membrane, while P-selectin expression is a hallmark marker of activation (13, 39). Annexin V binding, but not P-selection expression, was inhibited in the presence of GM6001 (Fig. 3 F). These data indicate that metalloproteinase-dependent cellular changes occurring during ESP generation leads to a reduced viability of these cells. Comparable results were obtained using a variety of different murine ESC lines (R1, EB3, TT2, or E14.1; unpublished data).

Inhibition of metalloproteinase activity restores integrin αIIbβ3 bidirectional signaling in ESPs

To explore whether metalloproteinases induce extracellular shedding of GPIbα and affect αIIbβ3 inside-out signaling, we used flow cytometry to assess specific fibrinogen binding upon agonist stimulation (9). GM6001 restored specific fibrinogen

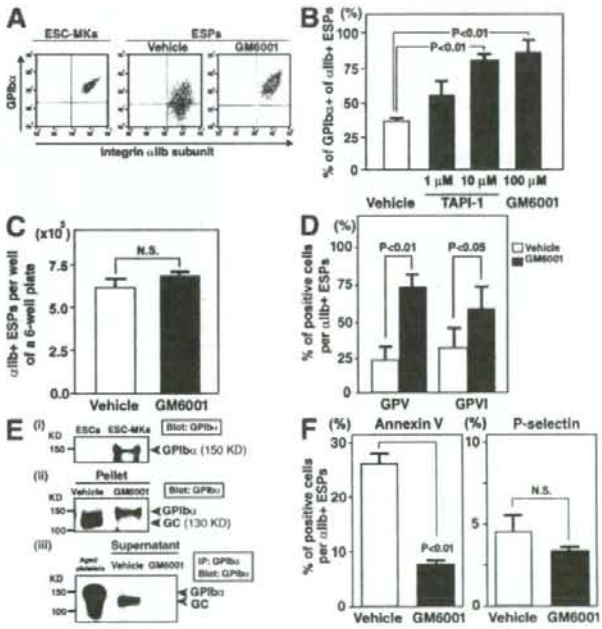

Figure 3. Inhibition of metalloproteinases in culture restores GPIbα expression in ESPs. (A) On day 10 of ESC culture, 1% DMSO alone (vehicle) or 100 μM GM6001 dissolved with 1% DMSO was added to the culture medium. On day 12 of culture, representative flow cytometry dot plots of mature megakaryocytes derived from ESCs (ESC-MKs) in the absence of GM6001 (left) and ESPs in the absence or presence of GM6001 are shown. (B) The graph shows the percentage of GPIbα$^+$ of all αIIb$^+$ ESPs on day 12 in the absence or presence of 1–10 μM TAPI-1 or 100 μM GM6001. Results are shown as mean ± SEM from three independent experiments. (C) The graph summarizes total numbers of αIIb$^+$ (αIIb$^+$GPIbα$^+$ plus αIIb$^+$GPIbα$^-$) ESPs per well of a 6-well plate on day 12. Results are the mean ± SEM from four independent experiments. (D) The graph shows the effects of the metalloproteinase inhibitor GM6001 on the surface expression of GPV or GPVI in αIIb$^+$ ESPs on day12. Results are mean ± SEM from four independent experiments. (E) Expression of GPIbα or GC in lysates from ESC-MKs (i), in lysates from pellets containing ESPs depleted of MKs (ii), or in supernatant (iii). In panel (i) or (ii), lysates were analyzed by Western blot (7.5% SDS-PAGE) with an anti-GPIbα antibody. In panel (iii), supernatant derived from culture media of ESPs pretreated with or without GM6001 were subjected to immunoprecipitation followed by immunoblotting with anti-GPIbα. In vitro–aged platelets from an adult mouse were used as a positive control in panel (iii). Similar results were obtained from three independent experiments. (F) The graphs show the percentage of positive cells of annexin V or P-selectin from the total αIIb$^+$ ESPs on day 12 in the absence or presence of GM6001. Results are the mean ± SEM from three independent experiments.

Published July 28, 2008

binding when washed ESPs were stimulated with thrombin or ADP (Fig. 4 A). To rule out the possibility that metalloproteinases directly impair integrin structure in ESPs, $MnCl_2$ was also used (40). Binding of Alexa 488–conjugated fibrinogen to ESPs was comparable in the presence or absence of GM6001 (Fig. 4 A) and similar to that in blood platelets (not depicted). Moreover, αIIbβ3-based actin cytoskeletal changes (outside-in signaling) of ESPs in culture were unexpectedly enhanced in the presence of GM6001, apparent when lamellipodia formation was facilitated by the addition of thrombin (Fig. 4 B, arrow). To address whether our observation of defects in ESPs also applied to blood platelets, we generated in vitro–injured human platelets by incubation at 37°C for 24 h. Reduced GPIbα expression was determined by flow cytometry and Western blot analysis (unpublished data), and a defect in lamellipodia formation in these aged platelets was observed. Impaired lamellipodia formation, apparent even upon thrombin stimulation, in aged human platelets was partially restored by the administration of GM6001 in culture for 24 h (Fig. S1, available at http://www.jem.org/cgi/content/full/jem.20071482/DC1). These data demonstrate that deregulated αIIbβ3-mediated bidirectional signaling (both inside-out and outside-in) may be associated with an increase in metalloproteinase activity in both ESPs and human platelets.

Metalloproteinases may regulate thrombus formation under flow conditions and posttransfusion recovery in vivo by ESPs

Thrombus formation is a dynamic process, and we sought to examine platelet function under physiologically relevant conditions found in the arterial circulation. An experimental system frequently used to study platelet thrombus formation is perfusion of whole blood over a monolayer of collagen at high shear rates, features mimicking those that occur in vivo (41). In this model, the initial event is tethering of platelets via binding of GPIbα to VWF, the latter being immobilized by collagen (10, 11, 13, 14). Direct interaction between integrin α2β1/GPVI on platelets and collagen follows (10). We prepared reconstituted whole blood consisting of mouse blood labeled with mepacrine, as a marker for platelets (green fluorescence), mixed (1,000:1) with Ds-red–labeled ESC-derived ESPs (red fluorescence). As a control, washed mouse platelets labeled with PE-conjugated anti-αIIb antibody were used (Fig. 5 A) (42). ESPs pretreated with 1% DMSO failed to adhere to collagen-VWF matrices, but pretreatment with GM6001 improved adhesion (Fig. 5, B and C). Most importantly, treating ESPs with GM6001-treated ESPs increased their ability to participate in thrombogenesis. However, their thrombus-forming potential was less than that of uninjured fresh platelets derived from adult mice (Fig. 5 C).

Aged or injured platelets are cleared out of the body after being trapped in the liver (unpublished data) and spleen (43). To confirm the effect of GM6001 on in vivo function of ESPs, we examined the time course kinetics of residual ESPs after transfusion. Because murine platelets do not express 1y5 antigen, we chose GFP-expressing ESCs for in vivo assays after transfusion (Fig. 6 A). More than 80% of ESPs on day 12

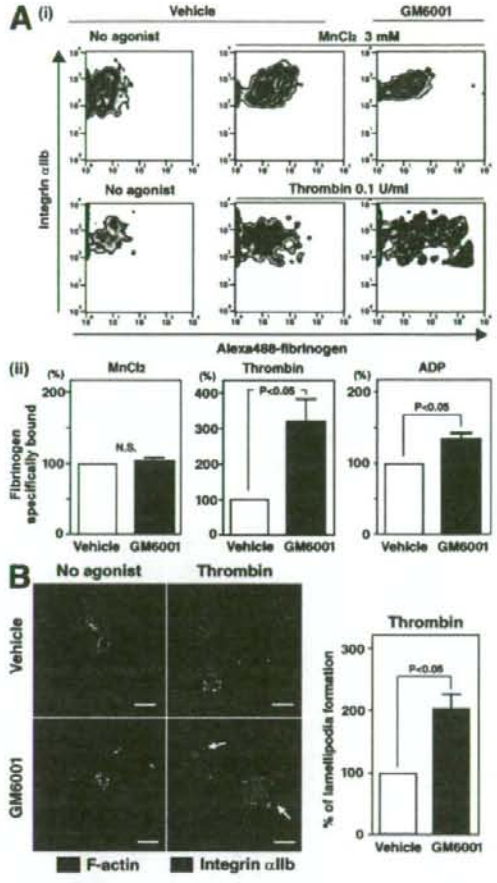

Figure 4. Inhibition of metalloproteinases is required for platelet function mediated through integrin αIIbβ3 in ESPs. (A) (i) Representative flow cytometry dot plots showing three mM $MnCl_2$-stimulated or 0.1 U/ml thrombin-stimulated fibrinogen binding to integrin αIIbβ3 in ESPs after pretreatment with 1% DMSO as a vehicle or 100 μM GM6001. (ii) The graphs show specific fibrinogen binding to αIIbβ3 stimulated with 3 mM $MnCl_2$ (reference 40), 0.1 U/ml thrombin, or 500 μM adenosine diphosphate. The value of control (vehicle) is defined as 100%. Results are the mean ± SEM from three independent experiments. (B) On day 14 of culture, washed ESPs pretreated with 1% DMSO or 100 μM GM6001 were plated on fibrinogen-coated coverslips for 45 min. An aliquot of each preparation was assayed in the presence of 1 U/ml thrombin. Cells were fixed, permeabilized, and stained with Alexa 488–phalloidin to stain F-actin (green) and with an anti-αIIb antibody followed by Alexa 567 (red). Bar, 10 μm. The value of control (vehicle) is defined as 100%. The right graph summarizes three independent experiments (mean ± SEM).

expressed GFP in culture. GM6001-treated ESPs were transfused into the tail veins of mice with significant thrombocytopenia (~10^4/μl) as a result of irradiation 10 d earlier (Fig. 6 A). 2, 24, 48, or 72 h after transfusion, whole blood was obtained from recipient mice, and the percentage of GFP-expressing platelets among all αIIb^+ platelets was determined.

Published July 28, 2008

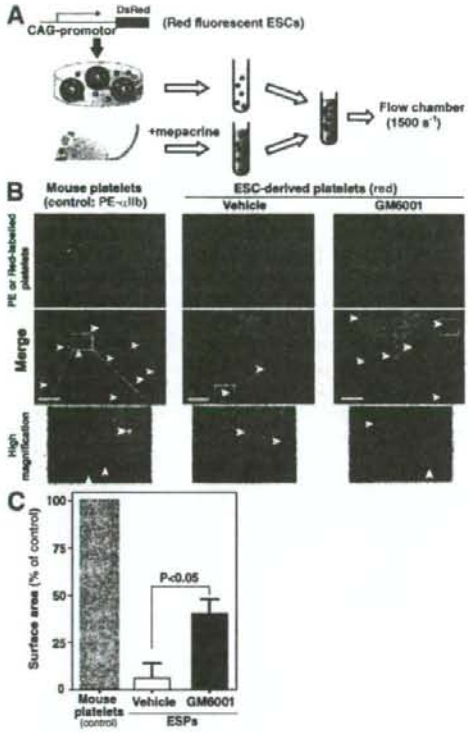

Figure 5. ESPs treated with GM6001 but not without GM6001 contribute to thrombus formation under flow conditions. (A) Schema of the experimental design. (B) Representative two-dimensional fluorescence images at 6 min. Glass slides coated with type I collagen were perfused at a wall shear rate of 1,500 s^{-1} for 6 min. Samples included reconstituted whole blood composed of ESPs (red, arrowheads) in blood obtained from 10–12 mice (per experiment), or a mixture of PE-labeled mouse platelets (red, arrowheads) in whole blood pooled from 10–12 mice. All murine platelets or ESPs were stained with mepacrine (green). ESPs capture fluorescent mepacrine as indicated by their dual expression of green and red by flow cytometer. Bars, 100 µm. (C) After 6 min, platelet thrombi formed on the collagen surface were quantified using NIH Images software from a recorded video. The results summarize four independent experiments (mean ± SEM).

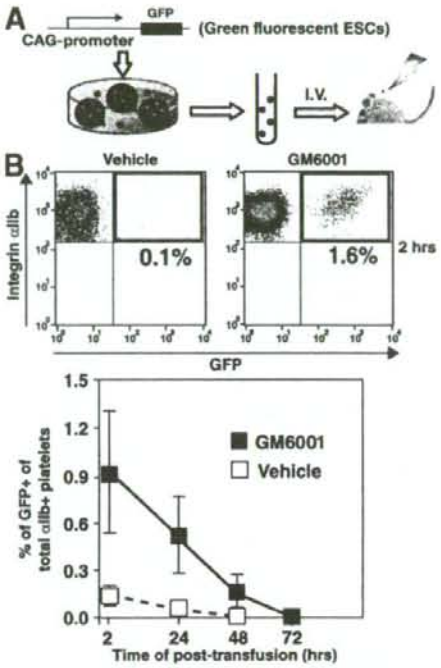

Figure 6. The effect of metalloproteinase inhibition on posttransfusion recovery by ESPs in mice. (A) Schema of the experimental design. (B) 2 h after transfusion of 3 × 10^6 ESPs, using a 129Ola strain mouse model in which platelet numbers are severely reduced, blood obtained from the retroorbital venous plexus was treated with 3.8% sodium citrate and subjected to flow cytometry to detect GFP+ platelets (ESPs) among all αIIb+ platelets. Additional serial evaluations were performed 24, 48, and 72 h after transfusion. Pretreatment with GM6001 increased the ratio of GFP+ ESPs per a recipient at all points examined. Results are the mean ± SEM from three independent experiments.

No difference in the size of endogenous platelets and ESPs transfused into recipient mice was observed (not depicted), suggesting that the in vivo circulation that may induce shear stress is an important determinant of platelet size (44). Preincubation with GM6001 consistently increased the percentage of GFP+ ESPs after transfusion compared with controls (Fig. 6 B).

DISCUSSION

This study has shown that (a) GPIbα, GPV, and GPVI, but not integrin αIIbβ3 or GPIbβ, are shed from ESPs during culture; (b) the process is specific for ESPs and not relevant for megakaryocyte differentiation from ESCs; (c) the use of a metalloproteinase inhibitor retains the complete GPIb–V-IX complex on ESPs; and (d) both inside-out and outside-in signaling of αIIbβ3 might be associated with metalloproteinase activity. A link between metalloproteinase regulation and αIIbβ3-mediated signaling has not been reported previously. Preventing shedding of the α-subunit of the GPIb–V-IX complex retains key binding sites for VWF, thrombin, coagulation factors, P-selectin, and Mac-1, all potentially important for normal platelet function (13). The N-terminal motif of GPIbα is essential for arterial thrombosis independent of VWF (12), and the signaling cascade from the GPIb–V-IX complex to αIIbβ3 is well known to regulate integrin activation (45). However, the mechanisms whereby metalloproteinase activity regulates integrin signaling remain to be identified.

Metalloproteinases are functionally regulated by endogenous inhibitors, the tissue inhibitors of metalloproteinases (TIMPs) (46). When we considered the reason why megakaryocytes maintained GPIbα in culture, as opposed to ESPs, we hypothesized that TIMP-3, also known to inhibit ADAM17 (47), might be highly expressed in megakaryocytes but not in

Published July 28, 2008

platelets (48). We therefore determined TIMP-3 expression in ESC-derived megakaryocytes and ESPs, but found no significant difference by RT-PCR (unpublished data). Alternatively, receptor shedding may be occurring with megakaryocytes but is not detectable owing to their gene and protein expression potential, which differs from the anucleate platelet (49).

Another interesting observation was that an administration of GM6001 or TAPI-1 from the beginning of culture impaired the production of c-Kit$^+$αIIb$^+$ cells by day 6 of the liquid culture (unpublished data). We observed that the use of inhibitors to metalloproteinases, which cover both MMPs and ADAMs, is advantageous for the production of efficacious platelets only after day 10 of co-culture. Nonspecific inhibition to metalloproteinases may affect the early phase of hematopoiesis from ESCs as demonstrated in postnatal hematopoiesis through MMP9-mediated mechanisms (50). In addition, it has been reported that MMP2 or MMP9 may have an effect on platelet function. MMP2 activates platelet aggregation through an increase in phospholipase C, protein kinase C, Ca^{2+} mobilization, and phosphatydylinositol 3 kinase (46, 51, 52). MMP9 blocks phospholipase C, protein kinase C, Ca^{2+} mobilization, and thromboxane A2 production leading to the inhibition of the effects of MMP2 (46, 52, 53). Integrins share some of these pathways and therefore might explain how both metalloproteinases and integrin activation might influence each other. In a search for specific MMPs regulating platelet function, we analyzed mice deficient in MMP9 and found comparable platelet numbers, integrin activation, and platelet spreading on fibrinogen comparing wild-type and MMP9-deficient mice (Fig. S2, A, C, and D, available at http://www.jem.org/cgi/content/full/jem.20071482/DC1). In addition, extracellular shedding of GPIbα was observed using in vitro–injured platelets from *MMP9*$^{-/-}$ mice as well as platelets from *MMP9*$^{+/+}$ mice (Fig. S2 B). These results indicate that MMP9 per se is not implicated in thrombopoiesis and platelet function.

Our results suggest that the administration of metalloproteinase inhibitors prolongs the half-life of circulating ESPs in vivo (Fig. 6), presumably by maintaining the repertoire of membrane receptors, such as GPIb-V-IX and GPVI. In patients with thrombocytopenia, platelet destruction is proportional to plasma concentrations of GC, a shedding product that includes the N-terminal domain of GPIbα (54). The ectodomain of GPIbα, GPV, and GPVI is easily shed in stocked human PCs possibly due to increased activities of ADAM17 and ADAM10 (12, 13, 55). Consistent with our study, GM6001 has been recently shown to prevent inactivation of refrigerated platelets by inhibiting ADAM17 activity (56). Specific inhibition to ADAM17 (and ADAM10) with spatial-temporal regulation not affecting hematopoiesis in ESCs may increase generation and storage of efficacious ESPs.

In conclusion, the inhibition of metalloproteinases in murine cultures of ESC-derived c-Kit$^+$αIIb$^+$ primitive cells represents an improvement in the production of efficacious ESPs. Confirming these observations starting with human cells is a future direction potentially defining an experimental framework to produce ESPs in sufficient quantity for clinical application.

MATERIALS AND METHODS

Plasmid preparation, reagents, and mice. All reagents were purchased from Sigma-Aldrich unless otherwise indicated. All animal and recombinant DNA experiments were approved by the Institutional Animal Care and Use Committee of the Institute of Medical Science, University of Tokyo. C57BL/6 mice were purchased from SLC. 129Ola mice (transfusion recipients) were purchased from The Jackson Laboratory. *MMP9*$^{-/-}$ mice were provided by Z. Werb (University of California, San Francisco, San Francisco, CA) (45). Rhodamine- and Alexa 488–conjugated phalloidin, Alexa 488–conjugated fibrinogen, Alexa 568–conjugated bovine IgG, and Alexa 647–conjugated mouse IgG antibodies were from Invitrogen. Purified human fibrinogen was from American Diagnostica Inc. FITC- and allophycocyanin (APC)-conjugated, PE-conjugated, and unconjugated anti-mouse integrin αIIb subunit and APC-conjugated anti-c-Kit, PE-conjugated anti-CD31, PE-conjugated anti-Sca-1, biotin-conjugated anti-CD9, FITC-conjugated anti-P-selectin, unconjugated human anti-GPIbα, and streptoavidin-APC–cyanine 7 (APC-Cy7) antibodies were from BD Biosciences. An annexin V-FITC apoptosis detection kit was purchased from BD Biosciences. PE-conjugated or unconjugated anti-mouse GPIbα, FITC-conjugated anti-mouse GPIbβ, GPV, GPVI, and GPIX antibodies were from Emfret. Biotin-conjugated anti-VE-cadherin antibody was provided by M. Ogawa (Kumamoto University, Kumamoto, Japan). Human TPO and erythropoietin were provided by H. Miyazaki (Kirin, Takasaki, Japan). Mouse leukemia inhibitory factor (ESGRO) was from Millipore. Human TPO, IL-6, and IL-11 were purchased from PeproTech. GM6001 and TAPI-1 (57) were from EMD.

Growth and differentiation of ES cells. The murine ESC lines E14tg2A (58), E14 (5), R1 (8), EB3 (37), and TT2 (7) were maintained as described previously (9). For EB formation, 2×10^5 ESCs were placed in 100-mm bacterial Petri dishes containing Iscove's modified Dulbecco's medium supplemented with a cocktail of 300 μg/ml human transferrin, 0.45 mM monothioglycerol, 50 μg/ml ascorbic acid, and penicillin-streptomycin/L-glutamine solution (Invitrogen). On day 5 or 6 of culture, cells were dissociated with 0.25% trypsin/EDTA and subjected to sorting by FACS MoFlo (Dako). Sorted cells (2×10^4 per well) were seeded onto OP9 stroma cells in 6-well plates with 20 ng/ml TPO as described previously (9). After 3 d of culture, a cocktail of 10 ng/ml TPO, 5 ng/ml IL-6, and 10 ng/ml IL-11 was added. Cell surface antigen expression was examined by flow cytometry (FACS Aria; BD Biosciences).

Establishment of GPIb-ESC line. An expression construct containing a human genomic DNA fragment containing the *GPIbα* promoter (28), followed by coding sequence for a human *GPIbα—EGFP* fusion, was inserted into pcDNA 3.1 (+)/zeo vector (Invitrogen). All sequences were subsequently confirmed by nucleotide sequencing. Completed pcDNA3.1 zeo vector was linearized with NheI site and transfected into E14tg2A ESCs by electroporation. After drug selection with 65 μg/ml zeocin for 7 d, resistant colonies were collected. Viable ESCs were confirmed by PCR to detect *zeocin* and human *GPIbα–EGFP* as a positive clone. To define useful ESC clones further, the intensity of GFP expression was assessed after differentiation into megakaryocytes (Fig. 1 C).

Quantification by RT-PCR. Sorted cells from day 6 EB or day 8 αIIb$^+$c-Kit$^-$ megakaryocytes cultured on OP9 were lysed with Trizol-LS (Invitrogen) for total RNA extraction. cDNAs were obtained by using Thermo Script RT-PCR System and oligo-dT primer (Invitrogen). Final results were normalized with intrinsic GAPDH and PCR Taqman PCR probe in quantity (Applied Biosystems). RT-PCR was performed to determine expression levels of genes of interest. Amplification proceeded for 30–39 cycles. PCR products were separated on agarose gels and visualized by ethidium bromide staining. The primer sets used are shown in Table S1, which is available at http://www.jem.org/cgi/content/full/jem.20071482/DC1.

ESP preparation and TEM study. Platelets in culture supernatant were gently collected. Acid citrate dextrose solution was added to yield final

Published July 28, 2008

concentrations of 8.5 mM sodium citrate, 6.5 mM citric acid, and 10.4 mM glucose. The collected fluid was centrifuged at 150 *g* for 10 min to eliminate large cells (e.g., megakaryocytes). The supernatant was transferred into a new tube, 1 μM prostaglandin E_1 and 1 U/ml apyrase were added to prevent platelet activation, and the mixture was centrifuged at 400 *g* for 10 min to sediment a platelet pellet. The pellet was resuspended in an appropriate volume of modified Tyrode-Hepes buffer, pH 7.4 (10 mM Hepes, 12 mM $NaHCO_3$, 138 mM NaCl, 5.5 mM glucose, 2.9 mM KCl, and 1 mM $MgCl_2$ without Ca^{2+}), or in 2% fetal bovine serum in PBS. To determine the number of platelets in culture, cells were mixed with True Count Beads (BD Biosciences). To detect ESPs in flow cytometry dot plots, the side scatter and forward scatter gates for murine plasma platelets (from mice aged 8–12 wk) were used. TEM studies were performed by using a JEOL 1200EX transmission electron microscope operating at 80 kV (JOEL). Specimens were treated with a mixture of 0.5% glutaraldehyde and 2% paraformaldehyde, followed by 1% osmium tetroxide for observation.

Biochemical studies. For immunoprecipitation, lysis buffer (2% Triton X-100 or 1% NP-40, 150 mM NaCl, 50 mM Tris-HCl, pH 7.4, 0.5 mM EGTA, 0.5 mM EDTA, 1 mM Na_3VO_4, 0.5 mM NaF, 0.5 mM PMSF, and 50 μg/ml leupeptin) was used. Separated supernatant in culture at day 12 of culture was immunoprecipitated with anti-GPIbα antibody and immunoblotted with anti-GPIbα antibody (clone Xia G7).

Integrin activation and actin cytoskeletal changes. To investigate integrin αIIbβ3 activation, 50-μl aliquots of ESPs were incubated with APC-conjugated anti-αIIb and 200 μg/ml Alexa 488–fibrinogen in the absence or presence of thrombin or ADP for 30 min at room temperature. Binding of Alexa 488–fibrinogen to ESPs was quantified using flow cytometry. Nonspecific binding was determined in the presence of 10 mM EDTA or 20 μg/ml 1B5, a specific inhibitor of mouse αIIbβ3 (provided by B. Coller, The Rockefeller University, New York, NY). Specific binding was defined as total minus nonspecific binding. To investigate outside-in signaling via αIIbβ3, all observations of cytoskeletal changes (morphology of spreading) in ESPs were performed using a confocal microscopic system (TCS SP2; Leica) as described previously (9).

Flow chamber study. To study the effect of inhibition on metalloproteinases, reconstituted whole blood was prepared by combining ESPs and mouse blood. ESPs were generated from ESCs in which the CAG promoter consistently controls Ds-red expression (provided by H. Niwa, RIKEN, Kobe, Japan) (Fig. 5 A). ESPs in which red fluorescent protein was expressed were combined (1:1,000 ratio) with mouse whole blood that had been labeled with mepacrine to mark mouse platelets; the total volume per experiment was 7–8 ml. Washed platelets obtained from mice aged 10–12 wk were stained with 4 μg/ml of PE-labeled anti-αIIb antibody (to avoid blocking effect) (42). This whole blood was also obtained from 11–12 C57/BL6 mice aged 10–12 wk per single experiment; argatrovan, an anti-thrombin drug (Mitsubishi Pharma), was added at a final concentration of 100 μM. Samples of the treated blood, containing ESPs, were injected into the chamber with a syringe pump (Harvard Apparatus) at a constant flow rate to achieve high wall shear rates (i.e., 1,500 s^{-1}) on collagen surfaces. Platelet thrombi forming on the collagen surfaces were visualized with an inverted-stage epifluorescence videomicroscope system (DM IRB; Leica) as described previously (59). The microscopic images were digitized online with a photosensitive color CCD camera (L-600; Leica). Image-J software (National Institutes of Health [NIH] Image) was used to quantify the percentages of surfaces covered by platelets.

Kinetics of residual ESPs in vivo after transfusion. ESPs were generated from ESCs in which the CAG promoter consistently controls GFP expression (provided by H. Niwa, RIKEN, Kobe, Japan) (Fig. 6 A). ESPs were generated in culture in the absence or presence of metalloproteinase inhibitor. On day 12 of culture, 3×10^6 ESPs were transfused into mice (129/Ola strain) in which platelet numbers had been reduced by irradiation (650 cGy) 10 d beforehand. To detect GFP-expressing ESPs at the indicated time points, blood samples were collected with micro-capillaries from the retro-orbital venous plexus and stained with APC-conjugated anti-αIIb antibody. The percentage of GFP^+ ESPs was determined by flow cytometry for each specimen.

Statistical analysis. Differences between experimental and control results (mean ± SE median) were analyzed by Student's *t* test. Probability values of $P < 0.05$ were considered significant.

Online supplemental material. Table S1 depicts the primers for Fig. 1 F. Fig. S1 shows the effects of GM6001 on the spreading of aged human platelets on fibrinogen. Fig. S2 shows the platelet number and functions via an integrin bidirectional signaling in *MMP9*$^{-/-}$ mice and their control *MMP9*$^{+/+}$ mice. The online supplemental material is available at http://www.jem.org/cgi/content/full/jem.20071482/DC1.

The authors thank Drs. H. Miyazaki, M. Ogawa, H. Niwa, B. Coller, and Z. Werb for providing reagents and mice. We are also very grateful to H. Tsukui for her excellent help and Drs. A.S. Knisely and M. Mahaut-Smith for manuscript review.

H. Nishikii, K. Eto, N. Tamura, T. Kanaji, A. Sawaguchi, and S. Goto performed the study. K. Hattori, B. Heissig, and J. Ware provided critical reagents. H. Nishikii and K. Eto designed the study. K. Eto and H. Nakauchi wrote the manuscript.

This work was supported by grants from the Ministry of Education, Culture, Sport, Science and Technology of Japan (to K. Eto and H. Nakauchi) and by a grant from Vehicle Locomotion Foundation (Tokyo, Japan, to K. Eto and S. Goto).

The authors have no conflicting financial interests.

Submitted: 18 July 2007
Accepted: 30 June 2008

REFERENCES

1. Webb, I.J., and K.C. Anderson. 1999. Risks, costs, and alternatives to platelet transfusions. *Leuk. Lymphoma.* 34:71–84.
2. McCullough, J. 2000. Current issues with platelet transfusion in patients with cancer. *Semin. Hematol.* 37:3–10.
3. Berger, G., D.W. Hartwell, and D.D. Wagner. 1998. P-Selectin and platelet clearance. *Blood.* 92:4446–4452.
4. Matsunaga, T., I. Tanaka, M. Kobune, Y. Kawano, M. Tanaka, K. Kuribayashi, S. Iyama, T. Sato, Y. Sato, R. Takimoto, et al. 2006. Ex vivo large-scale generation of human platelets from cord blood CD34+ cells. *Stem Cells.* 24:2877–2887.
5. Keller, G. 2005. Embryonic stem cell differentiation: emergence of a new era in biology and medicine. *Genes Dev.* 19:1129–1155.
6. Asano, T., K. Sasaki, Y. Kitano, K. Terao, and Y. Hanazono. 2006. In vivo tumor formation from primate embryonic stem cells. *Methods Mol. Biol.* 329:459–467.
7. van der Meer, P.F., and R.N. Pietersz. 2005. Gamma irradiation does not affect 7-day storage of platelet concentrates. *Vox Sang.* 89:97–99.
8. Fujimoto, T.T., S. Kohata, H. Suzuki, H. Miyazaki, and K. Fujimura. 2003. Production of functional platelets by differentiated embryonic stem (ES) cells in vitro. *Blood.* 102:4044–4051.
9. Eto, K., R. Murphy, S.W. Kerrigan, A. Bertoni, H. Stuhlmann, T. Nakano, A.D. Leavitt, and S.J. Shattil. 2002. Megakaryocytes derived from embryonic stem cells implicate CalDAG-GEFI in integrin signaling. *Proc. Natl. Acad. Sci. USA.* 99:12819–12824.
10. Ruggeri, Z.M. 2002. Platelets in atherothrombosis. *Nat. Med.* 8:1227–1234.
11. Nieswandt, B., and S.P. Watson. 2003. Platelet-collagen interaction: is GPVI the central receptor? *Blood.* 102:449–461.
12. Bergmeier, W., C.L. Piffath, T. Goerge, S.M. Cifuni, Z.M. Ruggeri, J. Ware, and D.D. Wagner. 2006. The role of platelet adhesion receptor GPIbalpha far exceeds that of its main ligand, von Willebrand factor, in arterial thrombosis. *Proc. Natl. Acad. Sci. USA.* 103:16900–16905.
13. Canobbio, I., C. Balduini, and M. Torti. 2004. Signalling through the platelet glycoprotein Ib-V-IX complex. *Cell. Signal.* 16:1329–1344.

14. Berndt, M.C., Y. Shen, S.M. Dopheide, E.E. Gardiner, and R.K. Andrews. 2001. The vascular biology of the glycoprotein Ib-IX-V complex. *Thromb. Haemost.* 86:178–188.
15. Rabie, T., A. Strehl, A. Ludwig, and B. Nieswandt. 2005. Evidence for a role of ADAM17 (TACE) in the regulation of platelet glycoprotein V. *J. Biol. Chem.* 280:14462–14468.
16. Bergmeier, W., C.L. Piffath, G. Cheng, V.S. Dole, Y. Zhang, U.H. von Andrian, and D.D. Wagner. 2004. Tumor necrosis factor-alpha-converting enzyme (ADAM17) mediates GPIbalpha shedding from platelets in vitro and in vivo. *Circ. Res.* 95:677–683.
17. Bergmeier, W., P.C. Burger, C.L. Piffath, K.M. Hoffmeister, J.H. Hartwig, B. Nieswandt, and D.D. Wagner. 2003. Metalloproteinase inhibitors improve the recovery and hemostatic function of in vitro-aged or -injured mouse platelets. *Blood.* 102:4229–4235.
18. Goto, S., N. Tamura, H. Ishida, and Z.M. Ruggeri. 2006. Dependence of platelet thrombus stability on sustained glycoprotein IIb/IIIa activation through adenosine 5′-diphosphate receptor stimulation and cyclic calcium signaling. *J. Am. Coll. Cardiol.* 47:155–162.
19. Shattil, S.J., and P.J. Newman. 2004. Integrins: dynamic scaffolds for adhesion and signaling in platelets. *Blood.* 104:1606–1615.
20. Takahashi, K., and S. Yamanaka. 2006. Induction of pluripotent stem cells from mouse embryonic and adult fibroblast cultures by defined factors. *Cell.* 126:663–676.
21. Hanna, J., M. Wernig, S. Markoulaki, C.W. Sun, A. Meissner, J.P. Cassady, C. Beard, T. Brambrink, L.C. Wu, T.M. Townes, and R. Jaenisch. 2007. Treatment of sickle cell anemia mouse model with iPS cells generated from autologous skin. *Science.* 318:1920–1923.
22. Nakorn, T.N., T. Miyamoto, and I.L. Weissman. 2003. Characterization of mouse clonogenic megakaryocyte progenitors. *Proc. Natl. Acad. Sci. USA.* 100:205–210.
23. Zhang, J., F. Varas, M. Stadtfeld, S. Heck, N. Faust, and T. Graf. 2007. CD41-YFP mice allow in vivo labeling of megakaryocytic cells and reveal a subset of platelets hyperreactive to thrombin stimulation. *Exp. Hematol.* 35:490–499.
24. Kyba, M., R.C. Perlingeiro, and G.Q. Daley. 2002. HoxB4 confers definitive lymphoid-myeloid engraftment potential on embryonic stem cell and yolk sac hematopoietic progenitors. *Cell.* 109:29–37.
25. Zhang, W.J., C. Park, E. Arentson, and K. Choi. 2005. Modulation of hematopoietic and endothelial cell differentiation from mouse embryonic stem cells by different culture conditions. *Blood.* 105:111–114.
26. Nakano, T., H. Kodama, and T. Honjo. 1994. Generation of lymphohematopoietic cells from embryonic stem cells in culture. *Science.* 265:1098–1101.
27. Nishikawa, S.I., S. Nishikawa, M. Hirashima, N. Matsuyoshi, and H. Kodama. 1998. Progressive lineage analysis by cell sorting and culture identifies FLK1+VE-cadherin+ cells at a diverging point of endothelial and hemopoietic lineages. *Development.* 125:1747–1757.
28. Hashimoto, Y., and J. Ware. 1995. Identification of essential GATA and Ets binding motifs within the promoter of the platelet glycoprotein Ib alpha gene. *J. Biol. Chem.* 270:24532–24539.
29. Ohmori, T., J. Mimuro, K. Takano, S. Madoiwa, Y. Kashiwakura, A. Ishiwata, M. Niimura, K. Mitomo, T. Tabata, M. Hasegawa, et al. 2006. Efficient expression of a transgene in platelets using simian immunodeficiency virus-based vector harboring glycoprotein Ibalpha promoter: in vivo model for platelet-targeting gene therapy. *FASEB J.* 20:1522–1524.
30. Lavenu-Bombled, C., B. Izac, F. Legrand, M. Cambot, A. Vigier, J.M. Masse, and A. Dubart-Kupperschmitt. 2007. Glycoprotein Ibalpha promoter drives megakaryocytic lineage-restricted expression after hematopoietic stem cell transduction using a SIN lentiviral vector. *Stem Cells.* 25:1571–1577.
31. Fujita, H., Y. Hashimoto, S. Russell, B. Zieger, and J. Ware. 1998. In vivo expression of murine platelet glycoprotein Ibalpha. *Blood.* 92:488–495.
32. Fraser, S.T., M. Ogawa, R.T. Yu, S. Nishikawa, M.C. Yoder, and S. Nishikawa. 2002. Definitive hematopoietic commitment within the embryonic vascular endothelial-cadherin(+) population. *Exp. Hematol.* 30:1070–1078.
33. Lepage, A., M. Leboeuf, J.P. Cazenave, C. de la Salle, F. Lanza, and G. Uzan. 2000. The alpha(IIb)beta(3) integrin and GPIb-V-IX complex identify distinct stages in the maturation of CD34(+) cord blood cells to megakaryocytes. *Blood.* 96:4169–4177.
34. Shivdasani, R.A. 2001. Molecular and transcriptional regulation of megakaryocyte differentiation. *Stem Cells.* 19:397–407.
35. Schulze, H., and R.A. Shivdasani. 2005. Mechanisms of thrombopoiesis. *J. Thromb. Haemost.* 3:1717–1724.
36. Tober, J., A. Koniski, K.E. McGrath, R. Vemishetti, R. Emerson, K.K. de Mesy-Bentley, R. Waugh, and J. Palis. 2007. The megakaryocyte lineage originates from hemangioblast precursors and is an integral component both of primitive and of definitive hematopoiesis. *Blood.* 109:1433–1441.
37. Lane, W.J., S. Dias, K. Hattori, B. Heissig, M. Choy, S.Y. Rabbany, J. Wood, M.A. Moore, and S. Rafii. 2000. Stromal-derived factor 1-induced megakaryocyte migration and platelet production is dependent on matrix metalloproteinases. *Blood.* 96:4152–4159.
38. Stephens, G., Y. Yan, M. Jandrot-Perrus, J.L. Villeval, K.J. Clemetson, and D.R. Phillips. 2005. Platelet activation induces metalloproteinase-dependent GP VI cleavage to down-regulate platelet reactivity to collagen. *Blood.* 105:186–191.
39. Clarke, M.C., J. Savill, D.B. Jones, B.S. Noble, and S.B. Brown. 2003. Compartmentalized megakaryocyte death generates functional platelets committed to caspase-independent death. *J. Cell Biol.* 160:577–587.
40. Nieswandt, B., M. Moser, I. Pleines, D. Varga-Szabo, S. Monkley, D. Critchley, and R. Fassler. 2007. Loss of talin1 in platelets abrogates integrin activation, platelet aggregation, and thrombus formation in vitro and in vivo. *J. Exp. Med.* 204:3113–3118.
41. Yap, C.L., K.E. Anderson, S.C. Hughan, S.M. Dopheide, H.H. Salem, and S.P. Jackson. 2002. Essential role for phosphoinositide 3-kinase in shear-dependent signaling between platelet glycoprotein Ib/V/IX and integrin alpha(IIb)beta(3). *Blood.* 99:151–158.
42. Falati, S., P. Gross, G. Merrill-Skoloff, B.C. Furie, and B. Furie. 2002. Real-time in vivo imaging of platelets, tissue factor and fibrin during arterial thrombus formation in the mouse. *Nat. Med.* 8:1175–1181.
43. Hoffmeister, K.M., T.W. Felbinger, H. Falet, C.V. Denis, W. Bergmeier, T.N. Mayadas, U.H. von Andrian, D.D. Wagner, T.P. Stossel, and J.H. Hartwig. 2003. The clearance mechanism of chilled blood platelets. *Cell.* 112:87–97.
44. Junt, T., H. Schulze, Z. Chen, S. Massberg, T. Goerge, A. Krueger, D.D. Wagner, T. Graf, J.E. Italiano Jr., R.A. Shivdasani, and U.H. von Andrian. 2007. Dynamic visualization of thrombopoiesis within bone marrow. *Science.* 317:1767–1770.
45. Kasirer-Friede, A., M.R. Cozzi, M. Mazzucato, L. De Marco, Z.M. Ruggeri, and S.J. Shattil. 2004. Signaling through GP Ib-IX-V activates alpha IIb beta 3 independently of other receptors. *Blood.* 103:3403–3411.
46. Santos-Martinez, M.J., C. Medina, P. Jurasz, and M.W. Radomski. 2007. Role of metalloproteinases in platelet function. *Thromb. Res.* 121:535–542.
47. Amour, A., P.M. Slocombe, A. Webster, M. Butler, C.G. Knight, B.J. Smith, P.E. Stephens, C. Shelley, M. Hutton, V. Knauper, et al. 1998. TNF-alpha converting enzyme (TACE) is inhibited by TIMP-3. *FEBS Lett.* 435:39–44.
48. Radomski, A., P. Jurasz, E.J. Sanders, C.M. Overall, H.F. Bigg, D.R. Edwards, and M.W. Radomski. 2002. Identification, regulation and role of tissue inhibitor of metalloproteinases-4 (TIMP-4) in human platelets. *Br. J. Pharmacol.* 137:1330–1338.
49. Zimmerman, G.A., and A.S. Weyrich. 2008. Signal-dependent protein synthesis by activated platelets: new pathways to altered phenotype and function. *Arterioscler. Thromb. Vasc. Biol.* 28:s17–s24.
50. Heissig, B., K. Hattori, S. Dias, M. Friedrich, B. Ferris, N.R. Hackett, R.G. Crystal, P. Besmer, D. Lyden, M.A. Moore, et al. 2002. Recruitment of stem and progenitor cells from the bone marrow niche requires MMP-9 mediated release of kit-ligand. *Cell.* 109:625–637.
51. Falcinelli, E., G. Guglielmini, M. Torti, and P. Gresele. 2005. Intraplatelet signaling mechanisms of the priming effect of matrix metalloproteinase-2 on platelet aggregation. *J. Thromb. Haemost.* 3:2526–2535.
52. Fernandez-Patron, C., M.A. Martinez-Cuesta, E. Salas, G. Sawicki, M. Wozniak, M.W. Radomski, and S.T. Davidge. 1999. Differential regulation of platelet aggregation by matrix metalloproteinases-9 and -2. *Thromb. Haemost.* 82:1730–1735.